ICT-619555 RESCUE

D2.1.2 Version 1.0

Final Report of The Coding/Decoding Algorithms and Performance Comparison

Contractual Date of Delivery to the CEC:	07/2016
Actual Date of Delivery to the CEC:	08/2016
Editor:	Valtteri Tervo
Authors:	Jiguang He, Xin He, Jiancao Hou, Weiwei Jiang, Sebastian Kühlmorgen, Tad Matsumoto, Anton Paatelma, Shen Qian, Valtteri Tervo, Albrecht Wolf, Na Yi
Participants:	JAIST, TUD, UNIS, UOULU
Work package:	WP2 – Code and algorithm design and optimization
Security:	**PU**
Nature:	**R**
Version:	1.0
Total number of pages:	54

Abstract: This deliverable provides comprehensive analytical and simulation results of the coding/decoding algorithms used in RESCUE. The algorithms are applied to various frameworks and investigated the applicability in selected cases. We also address the impact of lossy forwarding (LF) relaying in fading channels and specifically consider the evaluation of frame error rates (FERs) in comparison with lossless decode-and-forward (DF). Moreover, the deliverable proposes an algorithm for opportunistic relay selection in LF-based networks where the best relay can be found using a machine learning method. Remarkable performance gains are observed in a case where LF concept is applied in multi-antenna scenario, in which relays can transmit and receive at the same time by using multiple antennas for interference cancelation. Furthermore, we apply joint decoding (JD) into IEEE 802.11 WiFi standard. In addition, we present an error rate model for RESCUE physical layer to be used when designing higher layer protocols. After analyzing the results presented in this deliverable, we conclude that RESCUE concept is especially suitable for the cases where the retransmissions are not preferable or not even possible.

Keyword list: 802.11 WiFi, cooperative relaying, decode-and-forward, distributed turbo code, error rate model, iterative decoding, lossy forwarding, multiple antennas, wireless networks

Executive Summary

The RESCUE project – "Links-on -the-fly Technology for Robust, Efficient, and Smart Communication in Unpredictable Environments" – proposes a novel multi-route communication technology for multi-hop networks that are subject to dynamic topology changes. RESCUE is a cooperative communication paradigm consisting of decode-and-forward (DF) relaying that allows intra-link errors, combined with distributed turbo coding (DTC) that brings improved error protection. The relaying nodes decode and re-encode the data, and even with possible decoding errors, there exist correlation between the forwarded packet copies because they originate from the same source. Therefore, destination can improve the reliability of the detection by taking the correlation into account when decoding. The relaying method considered in RESCUE is referred as lossy forwarding (LF) which, in its original form, means that no integrity check is performed at the relay, but the frame is always forwarded. In this deliverable, we provide comprehensive analytical and simulation results of the coding algorithms used in RESCUE. Furthermore, we apply the coding algorithms to various frameworks and investigate its applicability in selected cases. The gains of the forward error correction (FEC) coding and joint decoding (JD) used in RESCUE are evident already from D2.1.1. Therefore, in this deliverable we also address the impact of LF relaying by comparing frame error rate (FER) results with the lossless counterpart that uses the same coding/decoding.

Firstly, we investigate a three-node system, referred as toy scenario 1 (TS1) defined in D1.2.1, by briefly introducing theoretical results considering the outage probabilities of different relaying strategies including a feedback-based strategy. Furthermore, we deeply investigate the differences between theoretical and practical simulation results, aiming at finding possible directions for improving the coding/decoding scheme. The second investigated case is a system with multiple relays without direct link, referred as toy scenario 2 (TS2), for which we show the superiority of LF compared with lossless forwarding in specific cases.

Opportunistic relaying is an attractive solution in order to reduce system complexity. In opportunistic relaying, the best relay is selected among available relay candidates according to a certain policy. It has been shown that there is no loss in performance in terms of the diversity-multiplexing tradeoff if only the best relay participates in cooperation. In this deliverable, we present an opportunistic relay selection strategy for LF system. Furthermore, a statistical learning method is proposed for practical implementations.

A successive single-input multiple-output (SIMO) erroneous relaying with iterative maximum *a posteriori* (MAP) receiver at destination is also proposed in order to allow relays' transmission and reception at the same time. In other words, one of the relays can transmit and the other receive resulting in the reduced multiplexing loss. The proposed scheme allows relays erroneously forward the decoded symbols, and jointly cancels interference and combines diversity at destination. It has been shown that, without extra cost of time delay and signalling overhead, the proposed scheme can exhibit up to 8 dB gain by comparing with the conventional selective DF (S-DF) based schemes.

An intuitive application of RESCUE contributions into current wireless standards is the use of JD in hybrid automatic repeat request (HARQ) to combine the retransmitted erroneous packets at the destination. In this deliverable, we report the results of applying JD into IEEE 802.11 WiFi standard. We show that with a minor changes, we can achieve performance improvements in terms of FER.

In order to efficiently evaluate and test the higher layer protocols, the abstraction in the physical layer (PHY) is needed. Therefore, we present an error rate model for RESCUE PHY, which is capable to accurately predict the link-level performance at low computational complexity and can therefore be utilized for the design and performance evaluation of algorithms and protocols that exploit DTC as well as for system-level simulation.

At the end, we find that LF is beneficial at least in the following cases:

1. Communications in rapidly changing network topology where the retransmissions are not possible.

2. Communications with low power devices where the nodes need to share the load with each other.

For FEC coding/decoding used in RESCUE, we can conclude that it is very simple but remarkably strong performing close to the theoretical limits. Therefore, it has a great potential to be applied in current wireless standards.

Authors

Partner	Name	E-mail / Phone
Japan Advanced Institute of Science and Technology (JAIST)	Tad Matsumoto Xin He Shen Qian Weiwei Jiang	matumoto@jaist.ac.jp hexin@jaist.ac.jp shen.qian@jaist.ac.jp wjiang@jaist.ac.jp
Technical University Dresden (TUD)	Sebastian Kühlmorgen Albrecht Wolf	sebastian.kuehlmorgen@tu-dresden.de albrecht.wolf@tu-dresden.de
University of Surrey (UNIS)	Jiancao Hou Na Yi	j.hou@surrey.ac.uk n.yi@surrey.ac.uk
University of Oulu (UOULU)	Valtteri Tervo Anton Paatelma Jiguang He	valtteri.tervo@ee.oulu.fi / +358 40 4167991 anton.paatelma@ee.oulu.fi jhe@ee.oulu.fi

Table of Contents

List of Acronyms and Abbreviations

Term	Description
16-QAM	16-ary quadrature amplitude modulation
ACC	Accumulator
ADF-JD	Adaptive decode-and-forward with joint decoding
ADF	Adaptive decode-and-forward
ANN	Artificial neural network
ARQ	Automatic repeat request
AWGN	Additive white Gaussian noise
BEP	Bit error probability
BER	Bit error rate
BICM	Bit interleaved coded modulation
BLER	Block error rate
BPSK	Binary phase shift keying
CBGF	Contention-based geographical forwarding
CC	Convolutional code
CCC	Constellation constrained capacity
CEO	Chief executive officer
CRC	Cyclic redundancy check
CSI	Channel state information
DF-JD	Conventional decode-and-forward with joint decoding (no lossy forwarding)
DF	Decode-and-forward
DTC	Distributed turbo coding
FEC	Forward error correction
FER	Frame error rate
FNN	Feedforward neural network
GI	Global iteration
HARQ	Hybrid automatic repeat request
HD	Half-duplex
HER	Header error rate
ID	Iterative decoding
JD	Joint decoding
LF	Lossy forwarding
LI	Local iteration
LLR	Log-likelihood ratio
MAC	Media access control
MAP	Maximum *a posteriori*
MCS	Modulation and coding scheme
MI	Mutual information
MRC	Maximal-ratio combining
MSP	Modified set partitioning
ODF	Opportunistic decode-and-forward (no lossy forwarding)
OFDM	Orthogonal frequency domain multiplexing
OLS	Opportunistic lossy forwarding
PCCC	Parallel concatenated convolutional codes
PHY	Physical layer
PSR	Packet success ratio
QPSK	Quadrature phase shift keying
RD	Relay-destination (sometimes can be written as R-D)
RESCUE	Links-on-the-fly Technology for Robust, Efficient, and Smart Communication in Unpredictable Environments
S-DF	Selective decode-and-forward
SD	Source-destination (sometimes can be written as S-D))
SCCC	Serial concatenated convolutional codes

SIMO	Single-input multiple-output
SINR	Signal-to-interference + noise ratio
SNR	Signal-to-noise ratio
SNRCC	Systematic non-recursive convolutional code
SOTA	State-of-the-art
SR	Source-relay (sometimes can be written as S-R))
SRCC	Systematic recursive convolutional code
TSx	Toy scenario x, $x = 1, 2$
USRP	Universal Software Radio Peripheral
V2I	Vehicle-to-infrastructure
V2V	Vehicle-to-vehicle

1. Introduction

The RESCUE project – "Links-on-the-fly Technology for Robust, Efficient, and Smart Communication in Unpredictable Environments" – aims at designing a communication network that is robust of sudden topological changes. Deliverable D1.1 [D11] defines two examples of such cases: public safety operations that take place in areas where the communication infrastructure is partially inoperable due to a disaster such as an earthquake, or vehicle-to-vehicle (V2V) communication, where cars and other vehicles share, for example, safety-critical information about the road and traffic conditions with each other.

RESCUE technology can be roughly characterized by two main factors: lossy forwarding (LF) and distributed turbo coding (DTC) for which the joint decoding (JD) is applied at the destination. In other words, RESCUE is a cooperative communication paradigm consisting of decode-and-forward (DF) relaying that allows intra-link errors, combined with DTC that brings improved error protection. The relaying nodes decode and re-encode the data, and the possible decoding errors at the relaying nodes result in correlation between the forwarded packet copies that the destination takes into account when decoding. LF in its original form means that no integrity check is performed at the relay, but the frame is always forwarded. Selective decode and forward (S-DF) [D121] can be viewed as a subcategory of LF, since S-DF uses a reliability criterion or threshold by which the forwarding decision is made. The basic principles of the RESCUE relaying strategy have been presented in [AM12; ZHA+12; ZCA+12].

In this deliverable, we apply RESCUE technology (LF and JD) in various cases in order to find out the indicators by which the RESCUE technology should be chosen for a certain application. It is intuitive that JD can improve the performance in any case, where multiple correlated packet copies are available at the destination. Furthermore, we find that LF is beneficial at least in the following cases:

- Communications in rapidly changing network topology where the retransmissions are not possible.
- Communications with low power devices where the nodes need to share the load with each other.

Communication networks are often designed by defining strict link budgets, which determines how the base stations are located around the target area. The link budget is affected by the limited maximum power that can be used for transmission, which in turn is regulated by local authority. Modulation and coding schemes (MCSs) should be also defined in such a way that we can have the best tradeoff in throughput and power consumption. When designing the MCSs for a fixed or slowly varying topology, it is not reasonable to aim at detection which is always error-free, since a large portion of the erroneous frames can be recovered by the automatic repeat request (ARQ) protocol. Hence, in such networks one should consider a tradeoff between transmit power, MCS and ARQ. The ARQ protocols developed specifically for RESCUE technology are described in [D31; D32; D33]. However, when the topology changes quickly, we cannot rely on ARQ. For example, when a car is passing by the relay nodes (fixed or mobile), there may be only one chance to send the information. If the information was received with errors, RESCUE technology can be used to recover it. Even if we would have a chance for retransmission from topology perspective, it is not always desirable. Such examples are the cases where the energy levels of the transmit and/or the receive nodes are low, and source nodes cannot afford of sending multiple times. In this case, it is not desirable to use only one link, but rather share the load with other nodes in order to increase the life time of the network.

The rest of the deliverable is organized as follows: In Chapter 2, we investigate LF in two different scenarios. We show that in a three-node system, referred as toy scenario 1 (TS1) defined in [D121], LF is superior to lossless forwarding when the retransmission from the source is not possible. The second investigated case is a system with multiple relays without direct link (TS2). In fading channel, depending on the channel realization, this scenario sometimes falls into the category of chief executive officer (CEO) problem, and sometimes there is multiple lossless frames to be provided from the relays. We show that LF can operate under difficult channel conditions where lossless forwarding fails. Chapter 3 presents an opportunistic relay selection strategy for LF system. Furthermore, a statistical learning method is proposed for practical implementations. A successive single-input multiple-output (SIMO) erroneous relaying with iterative maximum *a posteriori* (MAP) receiver at destination is proposed in Chapter 4. The proposed scheme allows relays erroneously forward the decoded symbols, and jointly cancels interference and combines diversity at destination. It has been shown that, without extra cost of time delay and signalling overhead, the proposed scheme can exhibit up to 8 dB gain by comparing with the conventional S-DF based schemes. Chapter 5 describes the application of JD for retransmitted frame copies into IEEE 802.11 a/g/p standard. It is shown that the performance can be improved with the expense of increased complexity at

the destination. The error rate model for RESCUE physical layer (PHY) is presented in Chapter 6. The model, referred as Blackbox, predicts the link-level performance at a low computational complexity and it has been used as a PHY abstraction in the work reported in [D32]. Finally, conclusions are drawn in Chapter 7 with the outlook on the directions of the future research work.

Literature Review on RESCUE Coding Algorithms

Distributed turbo codes was proposed in [VZ03]. Joint source-channel coding for two unknown correlated sources using channel codes and global iterations was presented in [GZ05]. They used turbo codes for both parallel branches resulting in the so called super turbo code. They also proposed a way to estimate the correlation at the destination in a case of two sources.

Performance of the successive coding strategy in the CEO problem was theoretically analyzed in [BS05]. An iterative joint decoding algorithm for the binary data gathering wireless sensor networks was proposed in [HBP08], where the convolutional code is applied as the coding scheme at the sensor node to protect the data transmitted over noisy links between the sensors and the fusion center. In [RYA11], a coding scheme based on the parallel concatenated convolutional codes (PCCC) was proposed. They used a joint decoding algorithm, which utilizes the correlation knowledge among the observations of the sensors by weighting the extrinsic log-likelihood ratios (LLRs) by the error probabilities of erroneous observations. Moreover, the capacity of the parallel channel was derived for verifying the bit error rate (BER) performance by taking into account the error probability of the observed data sequence. Recent work on the application of turbo trellis coded modulation on cooperative relaying is reported in [ABN+; ANH16].

In RESCUE, we apply the coding scheme from [PS06] to the relaying structure presented in [GZ05] and extend it to multiple correlated sources by using the approach in [HBP08]. In [D211; D23], we have proposed the novel decoding algorithm and carefully chosen the coding parameters including code polynomials, doping parameter values and mapping rules for binary phase shift keying (BPSK), quadrature PSK (QPSK) and 16-ary quadrature amplitude modulation (16-QAM), depending on the quality of the channels. All the functions have been implemented in C++, integrated to GNURadio system, and tested in simulations. Hence, this is a completely new code design and up to our best knowledge, there is no existing work with this extend. In top of the new coding scheme, multiple improvements for state-of-the-art (SOTA) correlation estimation algorithms have been proposed in [D211].

2. Study Cases on Lossy Forwarding

2.1 Introduction

The basic principles of RESCUE coding/decoding was presented in [D211]. We start by introducing a single frame encoder presented in Fig. 2.1 originally proposed in [PS06] for error floor removal in bit interleaved coded modulation (BICM) with iterative detection. First, a binary information sequence $\mathbf{u}$ is interleaved by an interleaver Π_1. Note that this interleaver is not necessary in point to point (P2P) communications. The purpose of Π_1 is to assure independent sources of extrinsic information for JD at the destination.

The first component code C, also referred as an outer code, is a systematic non-recursive convolutional code [Lee97]. Typically, in serial concatenated codes, the outer code is the stronger one (with lower code rate), however, it is not a necessary condition to obtain a good code. It is more like a result from the fact that the inner code is directly concatenated to the channel, which can be treated as a code itself.

After the convolutional code, the binary output sequence is interleaved and passed forward to the inner code. The inner code consists of two components: 1) a doped accumulator (ACC) [PS06], i.e., memory-1 systematic recursive convolutional code (SRCC), and 2) modulation mapper, which maps the bits to complex symbols according to a mapping rule $\mathscr{M}$. Inner doping [Ten01], in its original form, is used to trigger the convergence of a serial concatenated code by replacing some of the coded bits by uncoded bits. This is sometimes needed for non-systematic codes, which cannot produce enough extrinsic information without having any *a priori* information first. RESCUE uses the approach presented in [PS06], which is different compared to [Ten01]. The idea is to replace some of the uncoded bits by coded bits to enhance the error correction capability of the channel resulting in the disappearance of the error floor. The doping is characterized by a parameter P, which means that every P^{th} bit is taken from the ACC (encoded bit) and the rest are uncoded bits. The impact of the concatenation of ACC with mapper using various P values has also been investigated in [PS06]. In [PS06], they have also considered the impact of different mapping rules, which can significantly affect to the convergence properties of the system.

In [D211], the coding structure described above, is applied to DTC-LF, for which the JD is needed at the destination. Novel decoding algorithm was proposed with several correlation estimation strategies. In [D23], the physical layer implementation was described and the results of system level simulations were provided.

In this chapter, we further analyze the coding/decoding structure. Specifically, we address the situations where LF can extend the operational range of the network. In other words, if there are errors at the relay, LF relay forwards and lossless relay does not. Hence, the comparisons made in this chapter, do not consider the overall resources consumed in the network. In Section 2.2, we briefly introduce some theoretical results for toy scenario 1 (TS1) considering different relaying strategies including a feedback-based strategy. Furthermore, we deeply investigate the differences between theoretical and practical simulation results, aiming at finding possible directions for improving the coding/decoding scheme. In Section 2.3, we investigate a case with three relays without direct link (TS2) and show that LF can help of operating in very difficult channel conditions. The availability of feedback channel is not analyzed in TS2.

2.2 LF in TS1

In this section, we compare the theoretical bounds of different relaying strategies with practical simulation results. The system model of TS1 is presented in Section 2.2.1. Outage probabilities of different relaying schemes are derived in Section 2.2.2. Finally, numerical results are shown and discussed in Section 2.2.3.

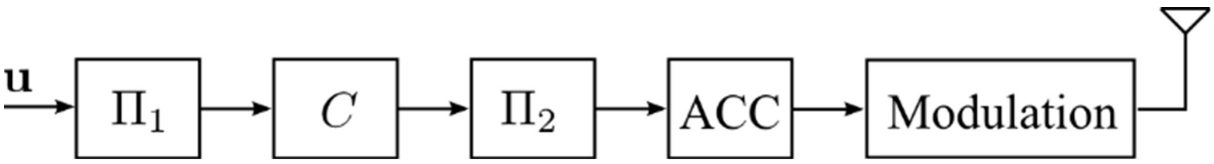

Figure 2.1.: Structure of the RESCUE encoder.

2.2.1 System and Channel Model

We consider a simple, three nodes relaying transmission model in a time-division channel allocation, as shown in Figure 2.2. A source (S) broadcasts the information sequence $\mathbf{b}_S$ to a relay (R) and a destination (D) at the first time slot. In the second time slot, either S or R, or neither of them, transmits the message $\mathbf{b}_S$ or $\mathbf{b}_R$ to D, respectively. Three relaying strategies are considered: 1) LF relaying: R decodes, re-encodes the information and forwards the received information sequence to D no matter whether the S-R link error is detected or not; 2) conventional DF relaying: R keeps silent if error is detected after decoding; 3) Adaptive decode-and-forward (ADF) relaying: S retransmits if errors are detected after decoding at R.

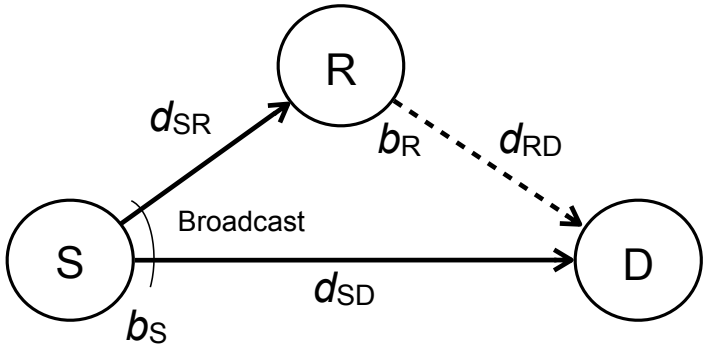

Figure 2.2.: One-way relaying transmission system.

The received signals y_1 via the S-D link and y_2 via the R-D link both at D, and the received signal y_3 via the S-R link at R are expressed as

$$y_1 = \sqrt{G_{\mathrm{SD}}} h_{\mathrm{SD}} x_1 + n_{\mathrm{SD}}, \tag{2.1}$$

$$y_2 = \sqrt{G_{\mathrm{RD}}} h_{\mathrm{RD}} x_2 + n_{\mathrm{RD}}, \tag{2.2}$$

$$y_3 = \sqrt{G_{\mathrm{SR}}} h_{\mathrm{SR}} x_1 + n_{\mathrm{SR}}, \tag{2.3}$$

respectively, where G_{ij} ($ij = \mathrm{SD}, \mathrm{RD}, \mathrm{SR}$) are the gains related to the distance of each link. h_{ij} and n_{ij} denote the complex channel gains and zero-mean additive white Gaussian noise (AWGN) with variance of $N_0/2$ per dimension, respectively. It is assumed that h_{ij} is constant over one block duration due to the block fading assumption. x_1 and x_2 denote the modulated symbols corresponding to the coded and interleaved information sequences, transmitted from S and R, respectively. The S-D, S-R, and R-D links are mutually independent with each other.

Let d_{SD}, d_{RD} and d_{SR} denote the distances between S and D, R and D, and S and R, respectively. The geometric gains of the S-R and R-D links, G_{SR} and G_{RD}, respectively, can be defined as

$$G_{\mathrm{SR}} = \left(\frac{d_{\mathrm{SD}}}{d_{\mathrm{SR}}}\right)^{\alpha}, G_{\mathrm{RD}} = \left(\frac{d_{\mathrm{SD}}}{d_{\mathrm{RD}}}\right)^{\alpha}, \tag{2.4}$$

where α is the path loss exponent. The gain G_{SD} of the S-D link is normalized to unity.

2.2.2 Outage Probability Analysis

In this section, the expressions of outage probability for various relaying protocols are derived. The outage is defined as that the information rate exceeds the capacity at corresponding signal-to-noise ratio (SNR). Let T_R and C_{ij} denote the threshold information rate and channel capacity of the ij link with Gaussian codebook assumption, respectively.

2.2.2.1 *Lossy Forwarding* (LF)

The information sequence, obtained as the result of decoding at R, is interleaved, re-encoded and transmitted to D, even if decoding errors are detected. The correlation knowledge between the information sequences transmitted from S and R is utilized in the iterative joint decoding process at D. The outage probability is defined as the probability that the source coding rate pair of S and R (R_S, R_R) falls into the inadmissible area A in Figure 2.3, or B or C in Figure 2.4. p_f represents the bit flipping probability between the information sequence obtained after decoding at R and the original sequence sent from S [ZCH+14], [QZH+ed].

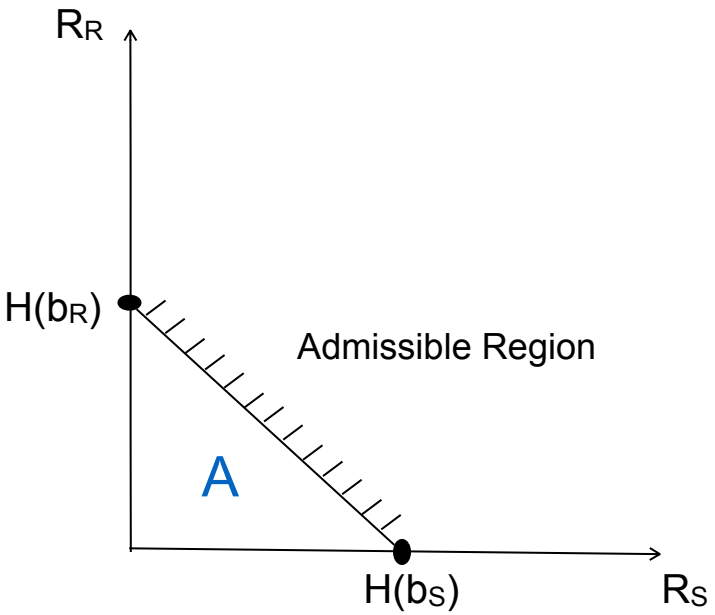

Figure 2.3.: Rate region for S and R when $p_f = 0$.

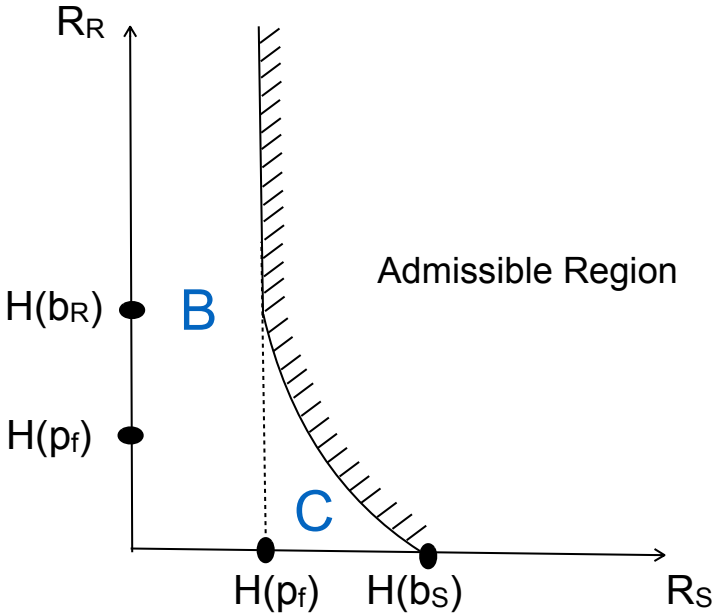

Figure 2.4.: Rate region for S and R when $p_f \neq 0$.

Let P_A, P_B, and P_C denote the probabilities that (R_S, R_R) falls into the inadmissible areas A, B, and C, respectively. According to the source coding with side information theorem [CT06, Section15.8], [GK11, Section10.4], the

outage probability of the LF relaying can be written as

$$\begin{aligned} P_{\text{out}}^{\text{LF}} =& P_{\text{A}} + P_{\text{B}} + P_{\text{C}} \\ =& \Pr[p_f = 0, 0 \le R_{\text{S}} < 1, 0 \le R_{\text{R}} < H(p'_f)], \\ &+ \Pr[0 < p_f \le 0.5, 0 \le R_{\text{S}} < H(p_f), R_{\text{R}} \ge 0], \\ &+ \Pr[0 < p_f \le 0.5, H(p_f) \le R_{\text{S}} < 1, 0 \le R_{\text{R}} < H(p_f * p'_f)]. \end{aligned} \tag{2.5}$$

where p'_f represent the crossover probability of the R-D link.

For calculating the outage probability, the relationships between γ_{SD} and R_{S}, and that between the instantaneous channel SNR of the R-D link γ_{RD} and R_{R} are established as

$$\gamma_{ij} \ge \Theta(R_k) = \left(2^{2R_k} - 1\right), (k = \text{S}, \text{R}), \tag{2.6}$$

according to Shannon's lossless source channel separation theorem.

The relationship between p_f and γ_{SR} can be established as

$$p_f = \Lambda(\gamma_{\text{SR}}) = H_2^{-1}\left(1 - \log_2(1 + \gamma_{\text{SR}})\right), \tag{2.7}$$

with the Hamming distortion measure. $H_2^{-1}(\cdot)$ denoting the inverse function of the binary entropy.

Then the outage probability of the LF relaying can be expressed as

$$P_{\text{A}} = \frac{1}{\overline{\gamma}_{\text{SD}}} \exp\left(-\frac{1}{\overline{\gamma}_{\text{SR}}}\right) \int_{\gamma_{\text{SD}}=\Theta(0)}^{\Theta(1)} \exp\left(-\frac{\gamma_{\text{SD}}}{\overline{\gamma}_{\text{SD}}}\right) \left[1 - \exp\left(-\frac{\Theta(1-\Theta(\gamma_{\text{SD}}))}{\overline{\gamma}_{\text{RD}}}\right)\right] d\gamma_{\text{SD}}, \tag{2.8}$$

$$P_{\text{B}} = \int_{\gamma_{\text{SR}}=\Theta(0)}^{\Theta(1)} \frac{1}{\overline{\gamma}_{\text{SR}}} \exp\left(\frac{\gamma_{\text{SR}}}{\overline{\gamma}_{\text{SR}}}\right) \left[1 - \exp\left(-\frac{\Theta(1-\Lambda(\gamma_{\text{SR}}))}{\overline{\gamma}_{\text{SD}}}\right)\right] d\gamma_{\text{SR}}, \tag{2.9}$$

and

$$P_{\text{C}} = \int_{\gamma_{\text{SD}}=\Theta(1-\Lambda(\gamma_{\text{SR}}))}^{\Theta(1)} \int_{\gamma_{\text{SR}}=\Theta(0)}^{\Theta(1)} \frac{1}{\overline{\gamma}_{\text{SD}}} \exp\left(\frac{-\gamma_{\text{SD}}}{\overline{\gamma}_{\text{SD}}}\right) \frac{1}{\overline{\gamma}_{\text{SR}}} \exp\left(\frac{\gamma_{\text{SR}}}{\overline{\gamma}_{\text{SR}}}\right) \left[1 - \exp\left(\frac{\Theta[\xi(\gamma_{\text{SD}}, \gamma_{\text{SR}})]}{\overline{\gamma}_{\text{RD}}}\right)\right] d\gamma_{\text{SD}} d\gamma_{\text{SR}}, \tag{2.10}$$

where $\xi(\gamma_{\text{SD}}, \gamma_{\text{SR}}) = H\{H^{-1}[1 - \Theta(\gamma_{\text{SD}})] * H^{-1}[1 - \Lambda(\gamma_{\text{SR}})]\}$.

*2.2.2.2 Conventional Decode-and-Forward with Joint Decoding (*DF-JD*)*

In the conventional DF relaying, S broadcasts the coded information sequence to D and R at the first time slot. If the transmitted information is successfully recovered at R, the information sequence is forwarded to D at the second time slot. R keeps silent if error is detected after decoding at R. A joint decoding process is performed to combine the signals received from S and R. The outage probability of the conventional DF relaying is defined as

$$P_{\text{out}}^{\text{DF-JD}} = \Pr\{T_R > C_{\text{SD}}(\gamma_{\text{SD}}) | T_R > C_{\text{SR}}(\gamma_{\text{SR}})\} \Pr\{T_R > C_{\text{SR}}(\gamma_{\text{SR}})\} + P_{\text{A}}. \tag{2.11}$$

The outage probability can be calculated as

$$\begin{aligned} P_{\text{out}}^{\text{DF-JD}} =& \left(1 - \exp\left(\frac{2^{T_R} - 1}{\overline{\gamma}_{\text{SR}}}\right)\right) \left(1 - \exp\left(-\frac{2^{T_R} - 1}{\Gamma_{\text{SD}}}\right)\right) \\ &+ \frac{1}{\overline{\gamma}_{\text{SD}}} \exp\left(\frac{1}{\overline{\gamma}_{\text{SR}}}\right) \int_{\gamma_{\text{SD}}=\Theta(0)}^{\Theta(1)} \exp\left(-\frac{\gamma_{\text{SD}}}{\overline{\gamma}_{\text{SD}}}\right) \left[1 - \exp\left(\frac{\Theta(1-\Theta(\gamma_{\text{SD}}))}{\overline{\gamma}_{\text{RD}}}\right)\right] d\gamma_{\text{SD}}. \end{aligned} \tag{2.12}$$

2.2.2.3 *Adaptive DF with Joint Decoding (*ADF-JD*)*

In ADF-JD transmission, S broadcasts the coded information sequence to D and R at the first time slot. If the transmitted information is successfully recovered at R, the information sequence is forwarded to D at the second time slot. The difference compared to conventional DF is that if the S-R transmission fails, S retransmits to D. D performs joint decoding to retrieve the original message of S. The information sequence is interleaved before forwarding to D from R when S-R transmission is successful, and also interleaved before retransmission from S when S-R retransmission fails. The rate region of ADF-JD is shown in Figure 2.5 and Figure 2.6. Similar as the case of LF, the outage probability is defined as the probability that the source coding rate pairs of S and R (R_S, R_R) and (R_S, R'_S) fall into the inadmissible area D or E shown in Figure 2.5 and Figure 2.6, respectively. R'_S is the rate of retransmitted information sequence from S.

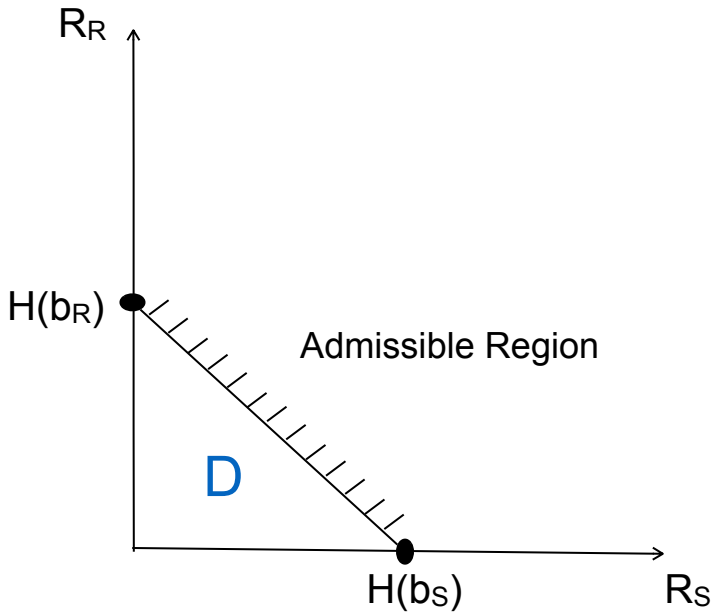

Figure 2.5.: Rate region for S and R when $p_f = 0$.

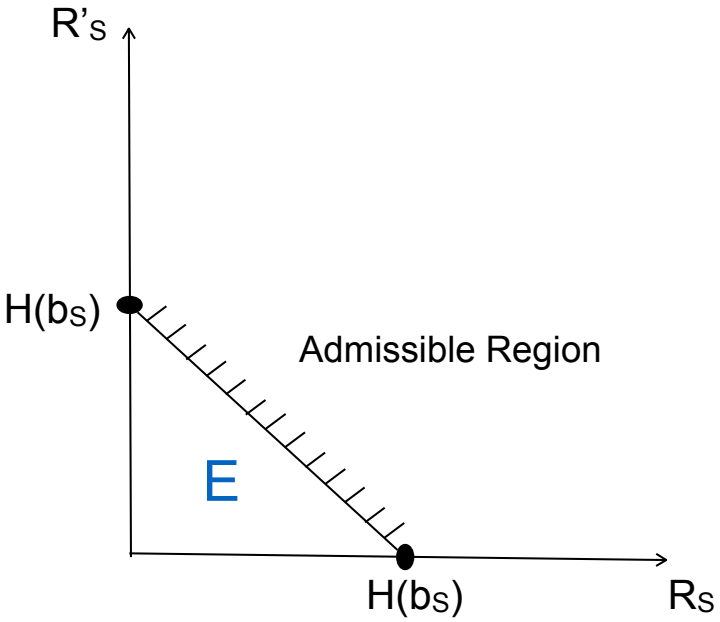

Figure 2.6.: Rate region for S and S' when $p_f \neq 0$.

Let P_{D} and P_{E} denote the probabilities that (R_{S}, R_{R}) and (R_{S}, R'_{S}) falls into the inadmissible areas D and E, respectively. The outage probability of ADF-JD can be defined as

$$\begin{aligned} P_{\mathrm{out}}^{\mathrm{ADF-JD}} =& P_{\mathrm{D}} + P_{\mathrm{E}} \\ =& \Pr[p_f = 0, 0 \le R_{\mathrm{S}} < 1, 0 \le R_{\mathrm{R}} < H(p_f)], \\ &+ \Pr[0 < p_f \le 0.5, 0 \le R_{\mathrm{S}} < 1, 0 \le R'_{\mathrm{S}} < H(p_f)]. \end{aligned} \tag{2.13}$$

Then, the outage probability can be calculated as

$$\begin{aligned} P_{\mathrm{out}}^{\mathrm{ADF-JD}} =& \frac{1}{\overline{\gamma}_{\mathrm{SD}}} \left(1 - \exp\left(\frac{1}{\overline{\gamma}_{\mathrm{SR}}}\right)\right) \int_{\gamma_{\mathrm{SD}}=\Theta(0)}^{\Theta(1)} \exp\left(-\frac{\gamma_{\mathrm{SD}}}{\overline{\gamma}_{\mathrm{SD}}}\right) \left[1 - \exp\left(\frac{\Theta(1-\Theta(\gamma_{\mathrm{SD}}))}{\overline{\gamma}_{\mathrm{RD}}}\right)\right] d\gamma_{\mathrm{SD}} \\ &+ \int_{\gamma_{\mathrm{SD}}=\Theta(0)}^{\Theta(1)} \frac{1}{\overline{\gamma}_{\mathrm{SD}}} \left[1 - \exp\left(-\frac{\Theta(1-\Theta(\gamma_{\mathrm{SD}}))}{\overline{\gamma}_{\mathrm{SD}}}\right)\right] \left(1 - \exp\left(\frac{1}{\overline{\gamma}_{\mathrm{SR}}}\right)\right) \exp\left(-\frac{\gamma_{\mathrm{SD}}}{\overline{\gamma}_{\mathrm{SD}}}\right) d\gamma_{\mathrm{SD}}, \end{aligned} \tag{2.14}$$

with the feedback channel is assumed to be lossless and the latency of the feedback transmission is ignored.

2.2.3 Numerical Results and Discussion

In this section, we present the numerical results of the outage probability calculation and the frame-error-rate (FER) performance of the relaying strategies. Since our theoretical analysis assumes capacity achieving code, outage probability serves as a theoretical bound for FER obtained through simulations. It is worth noting that the goal of the RESCUE project is not link design but coverage extension by cooperative diversity. Therefore, we use x-axis as the S-D link SNR per transmission and the power consumed by the relay is not taken into account. However, the S-D link SNR defines the SNRs of all the other links due to geometric path loss assumption (2.4).

The threshold rate are set to $T_R = 0.5$ and, the path loss exponent is set to $\alpha = 3.52$ as in [YG11]. In the FER simulations, we use a serial concatenation of a non-recursive convolutional code with a generator polynomial $[3,2]_8$ and a doped-accumulator [D211]. The channel code rates are $1/2$ for both S and R and binary phase shift keying (BPSK) is used for modulation.

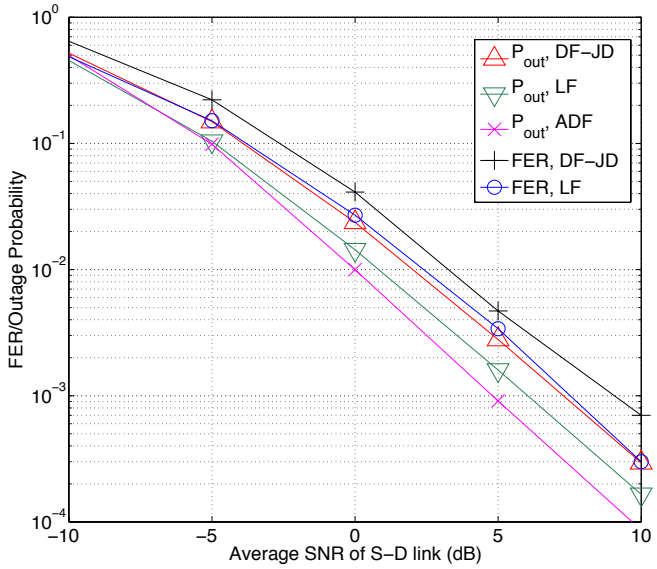

Figure 2.7.: Comparison of the outage probability of the LF, ADF, and the conventional DF system.

Figure 2.7 plots the theoretical outage probability versus average SNR of the S-D link, where all links are suffering from statistically independent block Rayleigh fading. The relay is at the midpoint between the source and the destination. It is found that the 2nd order diversity can be achieved at high SNR region by all the relaying strategies. As can be seen from the figure, LF relaying system can achieve better performance than the conventional DF system.

LF is about 1 dB better than conventional DF and 1 dB worse than ADF, respectively, at the outage probability of 0.001. The analytical results are very useful for evaluating the performance of practical code design for different protocols. The reason for ADF outperforming LF is that ADF has feedback information from R to tell S to retransmit when S-R transmission is failed. The admissible rate region of ADF in Figure 2.6 is increased compared to that of LF in Figure 2.4, which decreases the outage probability. It is found that the FER and their corresponding outage curves are consistent with each other, however, there are $1-2$ dB gaps in average SNR between the theoretical and simulation results. This is because the channel codes used are not capacity-achieving. The observation from simulation results indicates that the outage probability of LF relaying provides a better evaluation for the actual FER performance than that of conventional DF. It is worth of noticing that this comparison does not take into account the saved resources (time slots or power) in conventional DF if the relay cannot decode.

The impact of the relay location on the outage probability is depicted in Figure 2.8, where the average SNR of S-D link is kept at 5 dB. In this case, it is assumed that R is located on the line between S ($x = 0$) and D ($x = 1$). With the conventional DF (DF-JD) relaying system, the lowest outage probability is achieved at a certain point ($x \approx 0.4$) between S and the midpoint. An interesting observation is that as the relay is located at the midpoint (x = 0.5), the lowest outage probability can be achieved by LF relaying. In general, the lowest outage probability can be achieved at a point where the contributions of both S-R and R-D links to outage are balanced. Since in conventional DF, the relay stops forwarding the information sequence when errors are found, the quality of the S-R link has to be good enough, which results in the optimal position shifted closer to the side of the source. In LF system, the contributions of the two links to the outage probability are balanced because there is a chance that the errors occurring in the S-R link can be corrected at the destination, and as a consequence, the optimal location is the midpoint. With LF relaying the outage curve is symmetric with respect to the midpoint. The FER results have been obtained for two different relaying strategies presented in [D211]: 1) relay only extracts the systematic bits, then interleaves, encodes and transmits to destination; 2) relay performs full decoding, interleaves, encodes and transmits to destination. The FER curves exhibit almost the same tendency as the outage curve, except that the lowest FER performance is achieved at around 0.4. This is because the channel code used at S is not capacity-achieving and that causes a gap between the theoretical p_f value and the simulation result. It is also shown that the outage performance of LF relaying is superior to that of DF-JD relaying and inferior to that of ADF relaying.

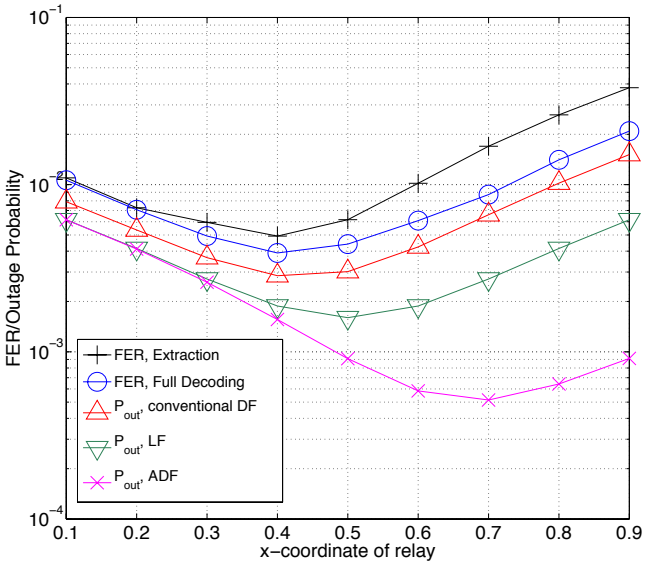

Figure 2.8.: Outage probability vs. the relay location, $\Gamma_{SD} = 5$ (dB)

2.3 LF in TS2

In this section, we show selected FER results for TS2, i.e., the case with source, three relays and destination. There is no direct link between the source and the destination and all the existing links are suffering from Rayleigh

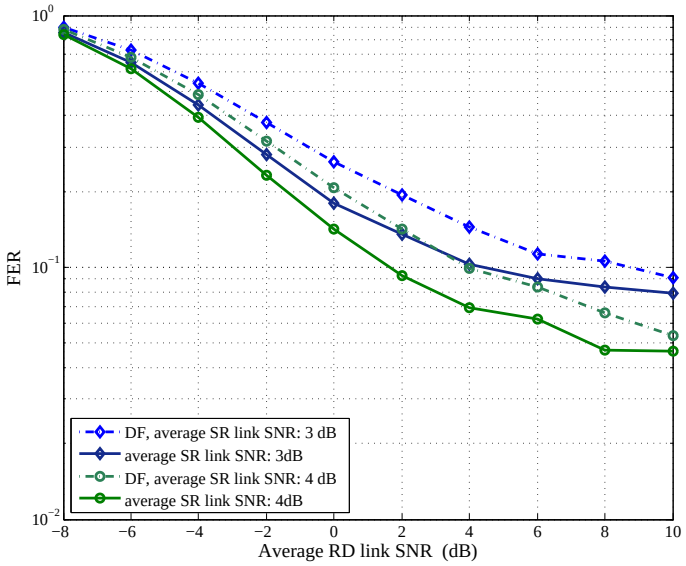

Figure 2.9.: FER vs. average SNR of RD links in a case with three relays. All the links are Rayleigh fading.

fading. We use a serial concatenation of a non-recursive convolutional code with a generator polynomial $[3,2]_8$ and a doped-accumulator with the doping rate 1. [D211]. The channel code rates are $1/2$ for both S and R and BPSK is used as a modulation. The block length is 1024 bits, and the maximum number of the local decoding iterations performed at the relay and destination is 3 and 25, respectively.

Firstly, we consider a case where the average SNRs of the links from source to relays (SR) are fixed. Moreover, we assume that the average SNRs of the SR links are the same. Then we obtain the FER values as a function of average SNR of relay-destination (RD) links. Here we also assume that the average SNRs of the RD links are the same. The results are shown in Fig. 2.9. We can observe that LF reduces FER through the whole SNR range considered. Here again reader should note that the comparison does not take into account the saved resources in conventional DF if the relay cannot decode.

In the other considered case we replace the SR links by bit flipping channel. Specifically, we have selected cases, for which there is high probability that all the relayed sequences are erroneous[1]. In a case of three relays, lossless forwarding can hardly operate due to the high probability of errors at the relays. The results are shown in Fig. 2.10. We can observe that FER less than 1 can be achieved even in the case where all the relayed sequences are erroneous with high probability. The case where all the relays can decode without errors is also plotted for comparison.

2.4 Conclusions

The performance of LF in terms of outage probability and FER has been investigated in this chapter. In case of TS1, we showed that our practical coding/decoding algorithm can reach very close to the theoretical limits. Furthermore, we showed that 1-2 dB gain can be achieved with LF compared to lossless DF in terms of FER and outage probability in Rayleigh fading environment. However, if the feedback link is available, ADF can yield the best performance among the algorithms tested. It is worth of noticing that in terms of the overall transmit power consumed in the network, the comparison between ADF and LF is fair unlike the comparison between DF-JD with LF or ADF. Therefore, if the nodes would be able to optimally adapt according to the links, LF does not introduce any gains in terms of the total transmit power in this simple network model. We could also observe from Fig. 2.7 that because the two time slots used in ADF were assumed to be always uncorrelated, all the considered strategies, ADF, LF and DF-JD can achieve the second order diversity. We also presented FER results for TS2 with various setups. We showed the superiority of LF compared to lossless DF in cases where the SNRs of the SR links are low.

[1]The smallest considered bit flipping value is 0.005 which means that 99.4% of the frames are erroneous with the block length of 1024.

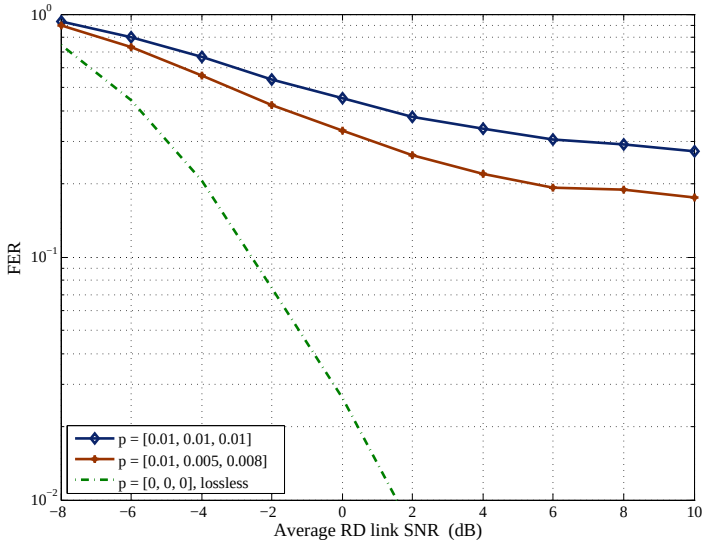

Figure 2.10.: FER vs. average SNR of RD links in a case with three relays. SR links assume bit flipping.

3. Opportunistic Relay Selection for Lossy-Forwarding

In this chapter, an opportunistic relay selection strategy for LF system is proposed. Furthermore, a statistical learning method is proposed for practical implementations.

3.1 System Model

The opportunistic LF system (OLF) model is depicted in Fig. 3.1, which contains one source S, one destination D and multiple relays R_i where $i \in \{1,...,m\}$. All links suffer from independent block Rayleigh fading, denoted by h_{SD}, h_{SR_i} and h_{RD_i} respectively. Hence, for each link, the channel can be expressed as $y = h \cdot s + n$, where s is the signal to be transmitted by the corresponding node, and n is the normalized noise with variance $\sigma^2 = N_0/2$.

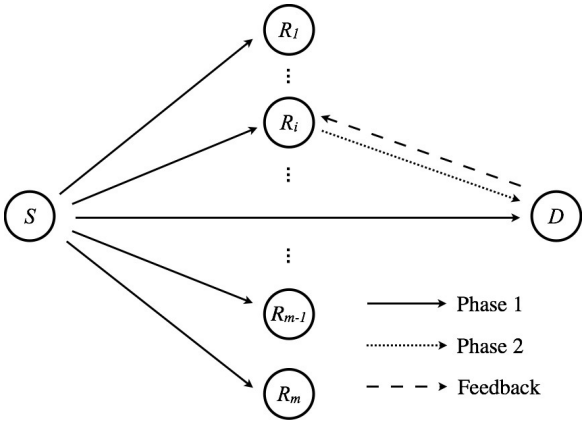

Figure 3.1.: Opportunistic LF system

The overall transmission involves $2+\varepsilon$ phases. In the first phase, the source node S broadcasts its signal to all other nodes, following a short ε phase for relay selection. In the second phase, only one relay R_i is selected and activated to help the transmission. The selected relay R_i is performed regardless of successful decoding, since the intra-link errors are allowed in our system. The destination node D jointly decodes the signals from the source node S and the selected relay R_i. The selection is made by the destination node D with the ε feedback phase. We assume that full channel state information (CSI) of each link is available at node D.

Furthermore, the source node S, the destination node D and the selected relay R_i composes a LF system [AM12] as shown in Fig. 3.2. The information of S, u_s, is encoded by using a serial concatenated convolutional code (SCCC). The received signal in relay is decoded, interleaved by an interleaver π, re-encoded by another SCCC encoder and transmitted to D. In the destination side, the signals from the source and the relay are jointly decoded. Function f_c is performed to prevent the error propagation due to the intra-link errors. We will use the same structure for our practical system simulations in section 3.4.

3.2 Outage Probability Calculation and Approximation

The objective of opportunistic relay selection is to minimize the outage probability for our system. To find the optimal selection strategy for our system, we first define the best relay R^* for each transmission as below

Definition 1. If R^* is selected and a transmission outage happens, then the transmission outage must happen $\forall R_j \in \{R_1,...,R_m\} \backslash R^*$.

Note that successful transmission is not guaranteed by the best relay. By *Definition 1*, the best relay R^* may not necessarily be single. Multiple relays can be candidates especially in higher signal-to-noise ratio (SNR) region, one relay from the candidates will be selected randomly in such scenarios.

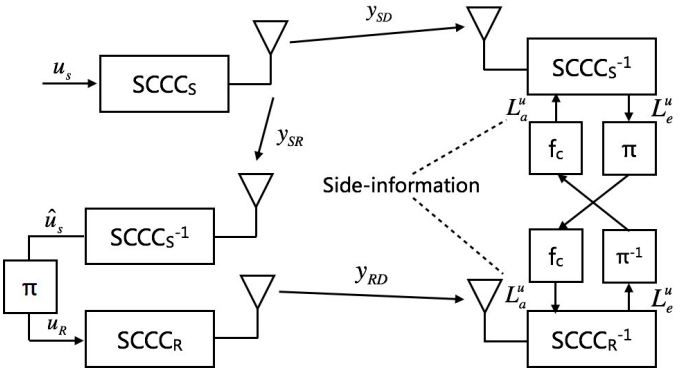

Figure 3.2.: System model of LF

According to *Definition 1*, the outage probability is defined as

$$\Pr(E|E_{R^*}) = \Pr[(E|E_{R_1}) \cap ... \cap (E|E_{R_m})], \tag{3.1}$$

where E is the overall outage event for a transmission, E_{R^*} is the event that the best relay is selected, and E_{R_i} is the event that relay R_i is selected. To calculate the exact outage probability, we can adopt the same technique proposed in [ZCH+14]. Since the events E_{R_i} are correlated to each other, we have to calculate the probability jointly. In [ZCH+14], the authors have calculated the outage probability by triple integrals corresponding to each link. In consequence, $2m+1$ multiple integrals are required to calculate the outage probability for OLF with m relays. The computation is intractable even when m is not large.

Therefore, we propose an approximated bound on outage probability based on Bayes's rule. Since the correlations among all the events E_{R_i} are due to the direct link, which infers that the correlations can be estimated by the outage probability for *SD* link that can be expressed as below by the Rayleigh fading assumption

$$\Pr(E_{SD}) = 1 - \exp(-\frac{\gamma_{th1}}{\Gamma_{SD}}), \tag{3.2}$$

where E_{SD} is the outage event of *SD* link, γ_{th1} is the threshold SNR and Γ is the average SNR of *SD* link. According to Bayes's rule, we can estimate equation (3.1) by

$$\begin{aligned}
\Pr(E|E_{R^*}) \approx & \Pr[\bigcap_{R_i \in S}(E|E_{R_i})|E_{SD}] \times \Pr(E_{SD}) \\
= & \prod_{R_i \in S} \Pr[(E|E_{R_i})|E_{SD}] \times \Pr(E_{SD}) \\
= & \frac{\prod_{R_i \in S} \Pr[(E|E_{R_i}), E_{SD}]}{\Pr^{m-1}(E_{SD})} \\
= & \frac{\prod_{R_i \in S} \Pr(E|E_{R_i})}{\Pr^{m-1}(E_{SD})}.
\end{aligned} \tag{3.3}$$

The last step is due to $E_{SD} \subseteq E|E_{R_i}$, and $\Pr(E|E_{R_i})$ is the LF outage probability with R_i and provided in [ZCH+14]. Numerical results are shown in Fig. 3.3 for two location configurations[1]. The gaps between the approximated theoretical bounds and Monte Carlo simulations, according to *Definition 1*, as the exact bounds, are around 0.5 dB for 2-relay system and 0.85 dB for 3-relay system. With theoretical bound, we have the proposition below.

Proposition 1. *The opportunistic LF system can achieve $m+1$ order diversity with m relays.*

Proof. According to [QCM15], in high SNR region, $\Pr(E|E_{R_i})$ can be approximated by

$$\Pr(E|E_{R_i}) \approx \frac{C_1}{\Gamma_{SD}^2} + \frac{C_2}{\Gamma_{SR^{(i)}}^2} + \frac{C_3}{\Gamma_{SR^{(i)}}\Gamma_{SD}} + \frac{C_4}{\Gamma_{SD}\Gamma_{RD^{(i)}}} \tag{3.4}$$

[1] In Location A, average SNRs are the same for all links; in Location B, relays are in the 1/4 point of the line from S to D, the average SNRs of Γ_{SR_i} and Γ_{RD_i} are $\Gamma_{SR_i} = \Gamma_{SD} + 10\log_{10}(4^{3.52})$ dB and $\Gamma_{RD_i} = \Gamma_{SD} + 10\log_{10}[(4/3)^{3.52}]$ dB. The spectrum efficiency for each node is 1.

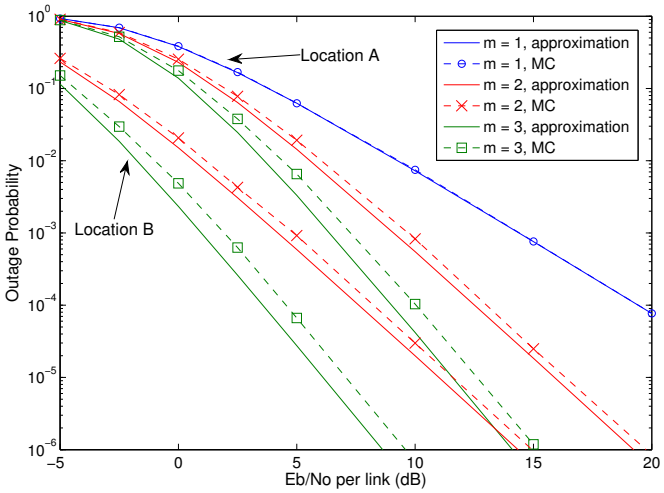

Figure 3.3.: Comparison between approximated theoretical outage probability bound and Monte Carlo simulations

where Γ_{SD}, $\Gamma_{SD^{(i)}}$ and $\Gamma_{RD^{(i)}}$ are the average SNRs for *SD*, *SR* and *RD* links with relay R_i respectively, and $C_1,\ldots,C_4$ are constants that are determined by spectrum efficiencies. The outage probability of *SD* link can also be approximated as

$$\Pr(E_{SD}) = 1-\exp(-\frac{\gamma_{th1}}{\Gamma_{SD}}) \approx \frac{\gamma_{th1}}{\Gamma_{SD}}, \tag{3.5}$$

by using the property that $e^{-x} \approx 1-x$ when x is small, implying high SNR region. Consequently, by assuming $\Gamma = \Gamma_{SD} = \Gamma_{SR_i} = \Gamma_{RD_i}$, when SNR goes to infinity, equation (3.3) can be expressed as

$$\begin{aligned}\Pr(E|E_{R^*}) \approx & (\frac{C_1+C_2+C_3+C_4}{\Gamma^2})^m \div (\frac{\gamma_{th1}}{\Gamma})^{m-1} \\ = & \frac{(C_1+C_2+C_3+C_4)^m}{\gamma_{th1}^{m-1}\Gamma^{m+1}}.\end{aligned} \tag{3.6}$$

Obviously $m+1$ order diversity can be achieved by equation (3.6). □

3.3 Relay Selection Strategy for Opportunistic LF

For the conventional opportunistic decode-and-forward (ODF) system where intra-link error is not allowed, R^* is given by

$$R^* = \arg\max_{R_i}\{\gamma_{R_i}\}, \tag{3.7}$$

where γ_{R_i} is the instantaneous SNR of R_i [HB07]. This is directly obtained by the fact that the maximal-ratio combining (MRC) performed by DF will take more advantage from higher SNR transmission of the relay. However, with intra-link errors, the story will be quite different. According to the theoretical analyses in [ZCH+14], the transmission over a LF system can be considered as source coding with side-information that is transmitted by the relay as showed in Fig. 3.2. Hence, to minimize the error after decoding, we want correlation between the side-information and the source information to be as high as possible. In the LF system, the correlation is reduced by the intra-link errors and the *RD* link errors, which means both *SR* and *RD* links have to be taken account equally. Therefore, the best relay R^* for our system is given by

$$R^* = \arg\min_{R_i}\{p_i * \alpha_i\}, \tag{3.8}$$

where p_i and α_i are the intra-link bit-error rates (BER) of *SR* and *RD* links respectively when R_i is selected, and $p_i * \alpha_i = (1-p_i)\alpha_i + p_i(1-\alpha_i)$. Point-to-point link BER p can be calculated from Shannon's lossy source-channel

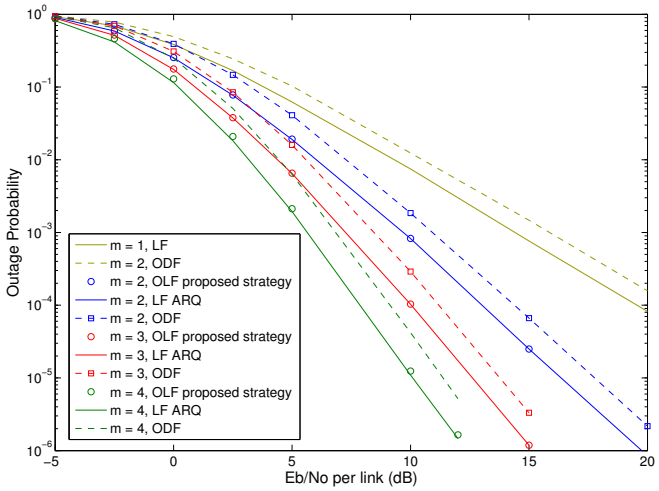

Figure 3.4.: Comparison of the theoretical outage probability of proposed opportunistic relay selection strategy, ARQ method and ODF system

separation theorem [ZCH+14]

$$p = \begin{cases} H_b^{-1}[1 - \dfrac{\log(1+\gamma)}{R_c}] & \gamma < \gamma_{th} \\ 0 & \gamma \geq \gamma_{th}, \end{cases} \tag{3.9}$$

where $H_b^{-1}(\cdot) : [0,1] \rightarrow [0,0.5]$ is the inverse binary entropy function, γ is the instantaneous SNR, and γ_{th} is the threshold SNR for coding rate R_c.

To verify our selection strategy, we conduct Monte Carlo simulations with $1,\ldots,4$ relays. For comparison, we propose an automatic repeat request (ARQ) scheme as the optimized case according to *Definition 1*. In the ARQ scheme, a relay is only activated when it receives an ARQ message. Whenever the destination node D cannot successfully decode, it sends an ARQ message to a randomly selected inactivated relay R_i to help the transmission. The process stops when the destination node D can successfully decode or all relays are activated. An outage happens when the destination cannot correctly decode the information from the source node S after all relays are activated. For fair comparison, decoding process in the destination restarts with the signal from the latest activated relay.

The numerical results in Fig. 3.4 indicate that the outage performance of proposed selection strategy is almost the same as the ARQ scheme for different relay numbers. The OLF outperforms conventional ODF system in the entire SNR region. In lower SNR region, the ODF outage probability is even higher than OLF with less number of relays. Though we assume symmetric channel here that the average SNR for each link is the same, the proposed selection strategy can also be used in asymmetric scenarios as the selection is based on instantaneous SNR.

3.4 Statistical Learning for Relay Selection

Our system can be implemented in various configurations especially for higher spectrum efficiency scenarios. For some specific system implements, the BER may be difficult to be estimated from the CSI, which is required for our theoretical selection strategy. In addition, the performance may also be impacted by some factors, such as block length, and undisclosed reasons. However, there may exist a hidden pattern to make the selection decision in specified system implementations. It is possible to build a practical selector without revealing such hidden patterns. In fact, the issue can be modeled as a typical classification problem that has been solved by statistical learning methods. For our system, the class is defined as the label of each relay (i for R_i), and the model aims to find the most possible label (best relay) given the inputs of instantaneous SNR.

We adopt a supervised machine learning method to select the best relay. In this paper, we utilize a simple fully

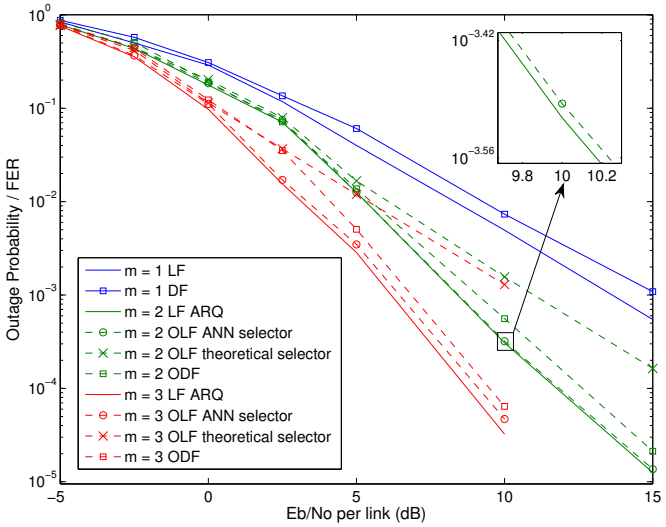

Figure 3.5.: FER performance of the ANN selector and the theoretical selector (BPSK)

connected 3-layer artificial neural network (ANN) for our system. To train an ANN selector for 2 relays, the numbers of nodes for input layer, hidden layer, and output layer are 5, 10, and 2 respectively. The type of ANN is feedforward neural network (FNN) [ABM08]. The objective function to find the optimized ANN selector Ω^* defined as

$$\Omega^* = \arg\max_{\Omega\in\Sigma}\{\mathbf{1}_{S_{R^*}}[\Omega(H)]\}, \tag{3.10}$$

where Σ is set of all possible ANN selectors. S_{R^*} and H are the set of best relays according to *Definition* 1 and the set of CSI for all transmission samples. The CSI we use only contains instantaneous SNR for each link.

To obtain the training data, we adopt traversal simulations for our system with 2 relays. The destination node D tries decoding jointly with each relay activated respectively. Transmission data are logged into a raw training data set $\mathscr{S}_{raw}$ as

$$\mathscr{S}_{raw} = \{\tau \mid \tau = \{S_C, h\}\}, \tag{3.11}$$

where S_C is the set of candidate relays with which the transmission outage does not happen, and h is the set of CSI of each transmission. Finally the valid training data set $\mathscr{S}$ is acquired by

$$\mathscr{S} = \{\tau \mid \tau \in \mathscr{S}_{raw}, |\tau[S_C]| = 1\}, \tag{3.12}$$

since the cases that the number of best relays is 2 or the transmission outage happens are not interesting for a relay selector.

With the trained ANN selector for 2 relays, selection for multiple relay scenarios can be performed recursively as

$$R^* = \Omega(\Omega(\Omega(R_2, R_1)..., R_{m-1}), R_m). \tag{3.13}$$

3.5 Numerical Results

In this section we demonstrate the simulation results for our proposed ANN selector compared with the optimal ARQ scheme, as well as with the selection strategy for conventional DF system. The common configurations are

- Information length: $n = 2000$

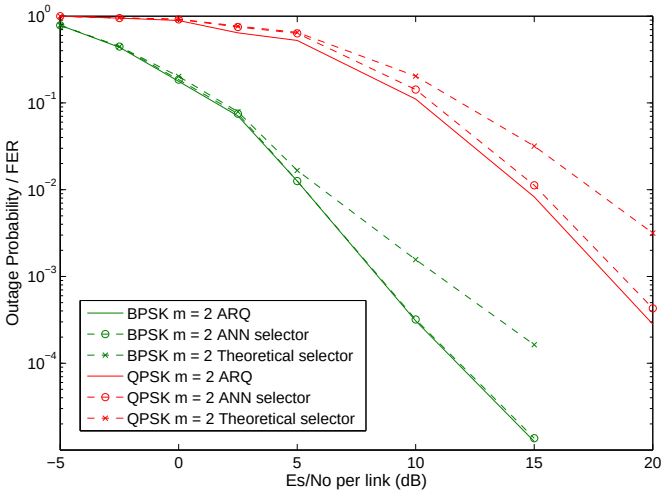

Figure 3.6.: Comparison between FER performance of proposed ODF selectors between BPSK and QPSK

- Interleavers: random
- Number of relays: 1, 2, and 3
- SCCC: a $[03, 02]_8$ half-rate non-recursive systematic convolutional code for outer coding, an accumulator with doping ratio 1 for inner coding.
- Modulation: binary phase-shift keying (BPSK) and quadrature phase-shift keying (QPSK) with gray mapping.
- Decoder: for proposed system, the numbers of iterations are 10 for SCCC and 30 for global iterations respectively. Intra-link error P_e is known. For conventional DF system, MRC is performed and the number of iterations is 10.

To train the ANN selector, 5658 items and 3622 items are fed for BPSK and QPSK respectively. The number of training iterations is 2000. The ratio of training data to test data is 7:3, and regularizing value λ for cost function is 0.5. Both training accuracy and test accuracy for BPSK are near 100%, while for QPSK are both beyond 90%.

Figs. 3.5 and 3.6 demonstrate the frame-error rate (FER) performance of the proposed ANN selector with BPSK and QPSK modulation and different numbers of relays. The result shows that the performance loss is very little compared to the optimal ARQ scheme. For m-relay scenarios, $m+1$ order diversity can be achieved. The theoretical selector based on equation (3.8) may work well in lower SNR region though, it may cause significant performance loss as the average SNR increases, and finally make the outage probability converge to the first order diversity for both 2-relay and 3-relay scenarios.

3.6 Conclusions

An opportunistic LF system was presented in this chapter. A machine learning method has been adopted for practical relay selection. Theoretical results and simulation results have shown that full diversity order can be achieved by the proposed system. Numerical results have indicated that our system outperforms conventional opportunistic decode-and-forward system in both theory and practice.

4. Successive SIMO Erroneous Relaying with Iterative MAP Receiver at Destination

4.1 Motivation and Objective

Successive single-input multiple-output (SIMO) relaying as one of promising cooperative communication schemes can be employed for the purpose of compensating multiplexing loss of conventional half-duplex (HD) constrained relaying [OS04; FWT+07]. Such scheme allows two HD relays alternately serve as transmitter and receiver to continuously transmit data frames for every channel use, and multiple receive antennas is used for interference cancellation. The optimal performance can be achieved if relays can perfectly decode source's messages. On the other hand, the performance is degraded if there exists decoding errors at relays. The authors in [WFT+09; HLT12] presented simple adaptive retransmission protocols to guarantee perfect decoding for relays at the cost of time delay and signalling overhead. Alternatively, the authors in [SZN11; BAP+14] used space-time codes to assist relays to mitigate inter-relay interference at cost of spectral efficiency especially for higher modulations.

In order to improve spectral efficiency and avoid error propagation effects, the successive relaying scheme can perform either conventional selective decode-and-forward (S-DF) relaying [WTG+11] or symbol-level selective transmission at relays [YMH+15]. At the first strategy, if any one of relays fails to correctly decode received frame, it will not transmit in the next time slot. Such procedure may largely lose diversity if relays always remain silent. At the second strategy, instead of discarding the whole frame after detecting decoding errors, relays predict correctly decoded symbols per frame based on a least-square principle and then forward them to destination to enjoy diversity. In this case, the complexity at relays is increased and prediction errors still exist.

Motivated by above observations, a successive SIMO erroneous relaying with iterative maximum a posteriori (MAP) receiver at destination is proposed, which aims to avoid high-complexity relays and improve both spectral efficiency and reliability. Specifically, with multiple receive antennas, relays firstly cancel inter-relay interference with QR decomposition, and then forward decoded frames regardless decoding errors. Following, destination performs the proposed iterative MAP receiver by taking the probability of decoding error at relays into account to jointly cancel interference and combine diversity. Here, the probability of decoding error at relays can be estimated and forwarded from relays as in [HYM15], or be directly estimated at the destination as in [GZ05]. Through simulations, it is shown that, without extra cost of time delay and signalling overhead, the proposed scheme exhibits up to 8 dB bit-error-rate performance gain by comparing with the conventional S-DF based relaying schemes.

4.2 System Model

Fig.4.1 illustrates the successive SIMO erroneous relaying with one source (S), two relays (R1/R2) and one destination (D). All transmissions are using single antenna, and all receptions are using two antennas. Assume discrete-

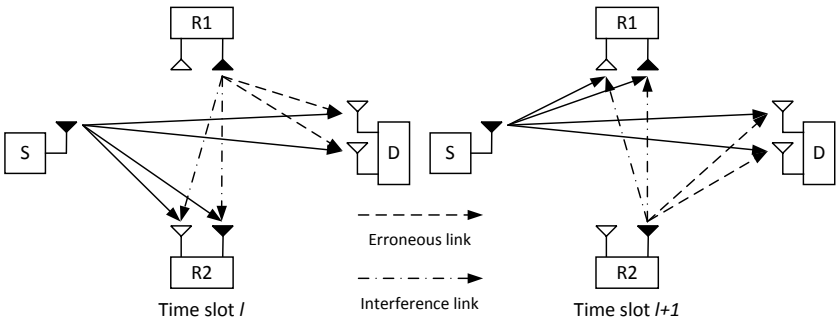

Figure 4.1.: Illustration of successive SIMO erroneous relaying.

time block fading channels, which remain static over each time slot. There are L frames being transmitted via $L+1$ time slots, where L is an even number. Source continuously transmits L frames in L time slots, and relays alternatively decode-and-forward received frames until the $(L+1)^{\text{th}}$ time slot. Here, in the 1^{st} time slot, only relay one and destination receive the 1^{st} frame from source, and in the $(L+1)^{\text{th}}$ time slot, only destination receives the L^{th} frame from relay two.

Let $\mathbf{Y}_{\mathrm{R}j}(l) \in \mathscr{C}^{2\times M}$ and $\mathbf{Y}_{\mathrm{D}}(l) \in \mathscr{C}^{2\times M}$ be the received signal matrices at the j^{th}, $j \in \{1,2\}$, relay, and at destination in the l^{th} time slot, respectively, where M is the number of symbols per frame. Thus, we have

$$\mathbf{Y}_{\mathrm{R}j}(l) = \mathbf{H}_{\mathrm{R}j}(l)\mathbf{X}(l) + \mathbf{V}_{\mathrm{R}j}(l), \tag{4.1}$$

$$\mathbf{Y}_{\mathrm{D}}(l) = \mathbf{H}_{\mathrm{D}}(l)\mathbf{X}(l) + \mathbf{V}_{\mathrm{D}}(l), \tag{4.2}$$

where $\mathbf{X}(l) \triangleq [\mathbf{x}_{\mathrm{R}\bar{j}}(l-1), \mathbf{x}_{\mathrm{S}}(l)]^T$ is the transmitted signal matrix in the l^{th} time slot composed by the $(l-1)^{\text{th}}$ frame from the $\bar{j}^{\text{th}}$, $\bar{j} \neq j \in \{1,2\}$, relay, i.e., $\mathbf{x}_{\mathrm{R}\bar{j}}(l-1) \in \mathscr{C}^M$, and the l^{th} frame from source, i.e., $\mathbf{x}_{\mathrm{S}}(l) \in \mathscr{C}^M$; $(\cdot)^T$ is transpose of a matrix; $\mathbf{H}_{\mathrm{R}j}(l) \in \mathscr{C}^{2\times 2}$ is the channel matrix from the $\bar{j}^{\text{th}}$ relay and source to the j^{th} relay in the l^{th} time slot; $\mathbf{H}_{\mathrm{D}}(l) \in \mathscr{C}^{2\times 2}$ is the channel matrix from the $\bar{j}^{\text{th}}$ relay and source to destination in the l^{th} time slot; $\mathbf{V}_{\mathrm{R}j}(l) \in \mathscr{C}^{2\times M}$ and $\mathbf{V}_{\mathrm{D}}(l) \in \mathscr{C}^{2\times M}$ are the additive white Gaussian noise (AWGN) matrices at the j^{th} relay and destination in the l^{th} time slot, respectively.

From (4.1) we can see, there exists inter-relay interference which should be cancelled before decoding the received frame from source. Such interference can be cancelled by QR decomposition without boosting noise power. Specifically, let $\mathbf{Q}_{\mathrm{R}j}(l) \in \mathscr{C}^{2\times 2}$ be the unitary matrix and $\mathbf{R}_{\mathrm{R}j}(l) \in \mathscr{C}^{2\times 2}$ be the upper triangular matrix generated from QR decomposition of the channel matrix $\mathbf{H}_{\mathrm{R}j}(l)$. Then, the received signal at the j^{th} relay after inter-relay interference cancellation is given by

$$\begin{aligned} \hat{\mathbf{Y}}_{\mathrm{R}j}(l) &= \mathbf{Q}_{\mathrm{R}j}^H(l)\mathbf{Y}_{\mathrm{R}j}(l), \\ &= \mathbf{R}_{\mathrm{R}j}(l) \begin{bmatrix} \mathbf{x}_{\mathrm{R}\bar{j}}^T(l-1) \\ \mathbf{x}_{\mathrm{S}}^T(l) \end{bmatrix} + \mathbf{Q}_{\mathrm{R}j}^H(l)\mathbf{V}_{\mathrm{R}j}(l), \end{aligned} \tag{4.3}$$

where $(\cdot)^H$ is hermitian of a matrix. Due to the structure of $\mathbf{R}_{\mathrm{R}j}(l)$, the desired signal after inter-relay interference cancellation is the second row of matrix $\hat{\mathbf{Y}}_{\mathrm{R}j}(l)$. In addition, due to the properties of $\mathbf{Q}_{\mathrm{R}j}(l)$, the noise power in (4.3) remains unchanged. After obtaining the desired signal, the j^{th} relay decodes and forwards it regardless decoding errors.

4.3 Iterative MAP Receiver for Joint Interference Cancellation and Diversity Combining

The proposed iterative MAP receiver at destination can be formulated by a two-step iterative process: In step one, the modified MAP detection is implemented to jointly cancel interference and mitigate error propagation effects; While in step two, the soft information, which was provided by step one, is combined and used for turbo-like decoder, and then the decoder's output is fed back to the modified MAP detection for the next iteration. With above process, the interference generated at destination can be cancelled, meanwhile, diversity of the relaying scheme is also improved.

4.3.1 The Modified MAP Detection

In order to let the proposed receiver have capability of mitigating error propagation effects, we firstly needs to modify the conventional MAP detection by taking the probability of decoding error at relays into account. Such probability can either be estimated at relays and then forwarded to destination as in [HYM15], or be directly estimated at destination as in [GZ05]. In detail, start from converting (4.2) to the real-valued equivalent form. Let $\tilde{\mathbf{Y}}_{\mathrm{D}}(l) \in \mathscr{R}^{4\times M}$, $\tilde{\mathbf{X}}(l) \in \mathscr{R}^{4\times M}$, and $\tilde{\mathbf{V}}_{\mathrm{D}}(l) \in \mathscr{R}^{4\times M}$ be real matrices obtained from $\mathbf{Y}_{\mathrm{D}}(l)$, $\mathbf{X}(l)$, and $\mathbf{V}_{\mathrm{D}}(l)$, respectively, as

$$\tilde{\mathbf{Y}}_{\mathrm{D}}(l) = [\mathscr{R}(\mathbf{Y}_{\mathrm{D}}(l))^T, \mathscr{I}(\mathbf{Y}_{\mathrm{D}}(l))^T]^T, \tag{4.4}$$

$$\tilde{\mathbf{X}}(l) = [\mathscr{R}(\mathbf{X}(l))^T, \mathscr{I}(\mathbf{X}(l))^T]^T, \tag{4.5}$$

$$\tilde{\mathbf{V}}_{\mathrm{D}}(l) = [\mathscr{R}(\mathbf{V}_{\mathrm{D}}(l))^T, \mathscr{I}(\mathbf{V}_{\mathrm{D}}(l))^T]^T. \tag{4.6}$$

Additionally, let $\tilde{\mathbf{H}}_{\mathrm{D}}(l) \in \mathscr{R}^{4\times 4}$ denote the real matrix obtained from $\mathbf{H}_{\mathrm{D}}(l)$, as

$$\tilde{\mathbf{H}}_{\mathrm{D}}(l) = \begin{bmatrix} \mathscr{R}(\mathbf{H}_{\mathrm{D}}(l)) & -\mathscr{I}(\mathbf{H}_{\mathrm{D}}(l)) \\ \mathscr{I}(\mathbf{H}_{\mathrm{D}}(l)) & \mathscr{R}(\mathbf{H}_{\mathrm{D}}(l)) \end{bmatrix}. \tag{4.7}$$

Then, the real-valued equivalent form of (4.2) is given by

$$\tilde{\mathbf{Y}}_{\mathrm{D}}(l) = \tilde{\mathbf{H}}_{\mathrm{D}}(l)\tilde{\mathbf{X}}(l) + \tilde{\mathbf{V}}_{\mathrm{D}}(l). \tag{4.8}$$

For the known channels in AWGN, the optimization problem of the conventional MAP detection for the m^{th} symbols in the l^{th} time slot can be expressed as [VHK04]

$$\min_{\tilde{\mathbf{x}}^{(m)}(l)} \left[\underbrace{\|\tilde{\mathbf{y}}_{\mathrm{D}}^{(m)}(l) - \tilde{\mathbf{H}}_{\mathrm{D}}(l)\tilde{\mathbf{x}}^{(m)}(l)\|^2}_{\triangleq \Delta^{(m)}(l)} - \sum_{k=1}^{4} \log p(\tilde{x}_{k,m}^{(l)}) \right], \tag{4.9}$$

where $\tilde{\mathbf{x}}^{(m)}(l)$ and $\tilde{\mathbf{y}}_{\mathrm{D}}^{(m)}(l)$ are the m^{th} column of $\tilde{\mathbf{X}}(l)$ and $\tilde{\mathbf{Y}}_{\mathrm{D}}(l)$, respectively; $p(\tilde{x}_{k,m}^{(l)})$ is the probability of $\tilde{x}_{k,m}^{(l)}$ happening, where $\tilde{x}_{k,m}^{(l)}$ is the symbol in the k^{th} row of $\tilde{\mathbf{x}}^{(m)}(l)$. In this case, logarithm likelihood ratio (LLR) of the symbol in the k^{th} row of $\tilde{\mathbf{x}}^{(m)}(l)$ after MAP detection can be expressed as [VHK04]

$$L[\tilde{x}_{k,m}^{(l)} | \tilde{\mathbf{y}}_{\mathrm{D}}^{(m)}(l)] = \log \frac{\sum_{x:\tilde{x}_{k,m}^{(l)}=+1} e^{-\Delta^{(m)}(l) + \sum_j \log p(\tilde{x}_{j,m}^{(l)})}}{\sum_{x:\tilde{x}_{k,m}^{(l)}=-1} e^{-\Delta^{(m)}(l) + \sum_j \log p(\tilde{x}_{j,m}^{(l)})}}. \tag{4.10}$$

Here, $p(\tilde{x}_{k,m}^{(l)}), \forall k$, are independent because they are consist of symbols from different frames.

As we know, LLRs of the symbols in the 1st and 3rd rows of $\tilde{\mathbf{x}}^{(m)}(l)$ belong to the erroneously forwarded frame from one of relays. Thus, denote $p_e^{(l)}$ as the probability of decoding error at the relay in the l^{th} time slot, then in order to mitigate error propagation effects, we have

$$\begin{aligned} p(\hat{x}_{j,m}^{(l)} = +1) &= (1 - p_e^{(l)}) p(\tilde{x}_{j,m}^{(l)} = +1) + p_e^{(l)} p(\tilde{x}_{j,m}^{(l)} = -1), \\ p(\hat{x}_{j,m}^{(l)} = -1) &= (1 - p_e^{(l)}) p(\tilde{x}_{j,m}^{(l)} = -1) + p_e^{(l)} p(\tilde{x}_{j,m}^{(l)} = +1), \end{aligned}$$

where $p(\hat{x}_{j,m}^{(l)})$ denotes the modified probability of the symbol in the j^{th} row of $\tilde{\mathbf{x}}^{(m)}(l)$, and $j \in \{1,3\}$. Then, replacing $p(\tilde{x}_{j,m}^{(l)})$ with $p(\hat{x}_{j,m}^{(l)})$ in (4.10) for all cases if $j \in \{1,3\}$, LLRs of the symbols in the 2nd and 4th rows of $\tilde{\mathbf{x}}^{(m)}(l)$ (i.e. LLRs for the forwarded frame from S, where $k \in \{2,4\}$) can be modified as

$$L[\tilde{x}_{k,m}^{(l)} | \tilde{\mathbf{y}}_{\mathrm{D}}^{(m)}(l)] = \log \frac{\sum_{\tilde{x}:\tilde{x}_{k,m}^{(l)}=+1} e^{-\Delta^{(m)}(l) + \Theta^{(m)}(l)}}{\sum_{\tilde{x}:\tilde{x}_{k,m}^{(l)}=-1} e^{-\Delta^{(m)}(l) + \Theta^{(m)}(l)}}, \tag{4.11}$$

and LLRs of the symbols in the 1st and 3rd rows of $\tilde{\mathbf{x}}^{(m)}(l)$ (i.e. LLRs for the erroneously forwarded frame from one of relays, where $k \in \{1,3\}$) can be modified as

$$L[\tilde{x}_{k,m}^{(l)} | \tilde{\mathbf{y}}_{\mathrm{D}}^{(m)}(l)] = \log \frac{(1 - p_e^{(l)}) \sum_{\tilde{x}:\tilde{x}_{k,m}^{(l)}=+1} e^{-\Delta^{(m)}(l) + \Theta^{(m)}(l)} + p_e^{(l)} \sum_{\tilde{x}:\tilde{x}_{k,m}^{(l)}=-1} e^{-\Delta^{(m)}(l) + \Theta^{(m)}(l)}}{(1 - p_e^{(l)}) \sum_{\tilde{x}:\tilde{x}_{k,m}^{(l)}=-1} e^{-\Delta^{(m)}(l) + \Theta^{(m)}(l)} + p_e^{(l)} \sum_{\tilde{x}:\tilde{x}_{k,m}^{(l)}=+1} e^{-\Delta^{(m)}(l) + \Theta^{(m)}(l)}}. \tag{4.12}$$

Here, we have

$$\Theta^{(m)}(l) \triangleq \sum_{j, j \in \{2,4\}} \log p(\tilde{x}_{j,m}^{(l)}) + \sum_{j, j \in \{1,3\}} \log p(\hat{x}_{j,m}^{(l)}). \tag{4.13}$$

The derivation of (4.12) is trivial with similar procedure given in [LH09].

4.3.2 Iterative MAP Receiver at Destination

Unlike the work in [VHK04], where the iterative decoding is for multiple antenna point-to-point system and the transmitted frame in every time slot can be individually decoded, the proposed iterative MAP receiver for the

successive SIMO erroneous relaying needs to wait all L frames being received via $L+1$ time slots and then jointly decode those frames. Given the probability of decoding error at relays, as we described above, the proposed iterative MAP receiver at destination can be divided into a two-step iterative process: the modified MAP detection and the conventional turbo-like decoding.

The detailed iterative MAP receiver at destination is illustrated in Fig.4.2. In the l^{th} time slot, destination simul-

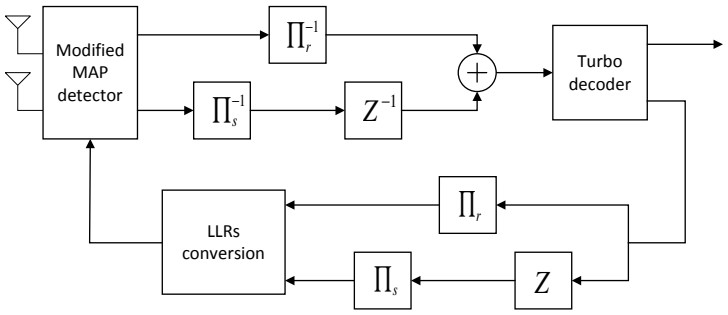

Figure 4.2.: The proposed iterative MAP recevier.

taneously receives the $(l-1)^{\text{th}}$ frame from one of relays and the l^{th} frame from source. Thus, the modified MAP detection can be implemented to cancel inter-frame interference and generate LLRs for these two frames based on (4.11) and (4.12). Such detection process continues until all L frames obtain two versions of LLRs from both relay and source. After that, the two versions of LLRs for each frame are separately deinterleaved and then combined for the turbo-like decoder. The extrinsic LLRs of the coded bits for each frame after the turbo-like decoder will be duplicated and separately interleaved for both relay and source. Following, the interleaved LLRs are converted to the probabilities $p(\tilde{x}_{k,m}^{(l)}), \forall k,m,l$, based on the modulator mapping function and then fed them back to the modified MAP detection for the next iteration use. In Fig.4.2, Π and Π^{-1} denote interleaving and deinterleaving, respectively; Z and Z^{-1} represent forward and backward shifting the frame number, respectively; "LLRs conversion" box is used to convert the interleaved LLRs to $p(\tilde{x}_{k,m}^{(l)}), \forall k,m,l$.

Remark 1: Similar as [VHK04], random interleavers implemented in Fig.4.2 and also in their corresponding transmitters are used to guarantee $p(\tilde{x}_{k,m}^{(l)}), \forall k,m,l$, to be independently distributed.

Remark 2: For $2 \leq l \leq L$ time slots, destination simultaneously receives two different frames from one of relays and source. In this case, the shifter Z is implemented to guarantee the same frame's LLRs being combined for the turbo-like decoder, and the shifter Z^{-1} is implemented to guarantee the adjacent frames' LLRs being converted into the probabilities at the same time for the modified MAP detection.

4.4 Simulation Results

Computer simulations were used to evaluate the bit-error-rate (BER) performance of the proposed successive SIMO erroneous relaying with iterative MAP receiver at destination. All channels were generated as independent block Rayleigh fading, which remained static over each transmission time slot. Assumed that there were $L = 20$ frames being transmitted via $L+1$ time slots, and no adaptive retransmission was considered. SNR denoted as the transmission power normalized by noise power ratio. The quadrature phase-shift keying modulation and turbo-like channel coding were also considered for the system. In detail, 1/2 rate serial concatenated convolutional code was used at source and relays, where the first encoder was the non-recursive non-systematic convolutional code with a generator polynomial $G = ([3,2])_8$, and the second encoder was the doped-accumulator with a doping rate equalling 2. Random interleavers were implemented, and simulation results were computed on an average over 10,000 independent channel realizations.

Four baselines were used for comparisons: 1) *Perfect decoding at relays*: this was served as BER performance bound, where relays can perfectly decode source's messages all the time and the same iterative decoding at destination as the proposed scheme; 2) *Proposed iterative decoding (ID) without* p_e: relays always forward decoded symbols regardless decoding errors but the iterative decoding at destination without taking p_e into account; 3)

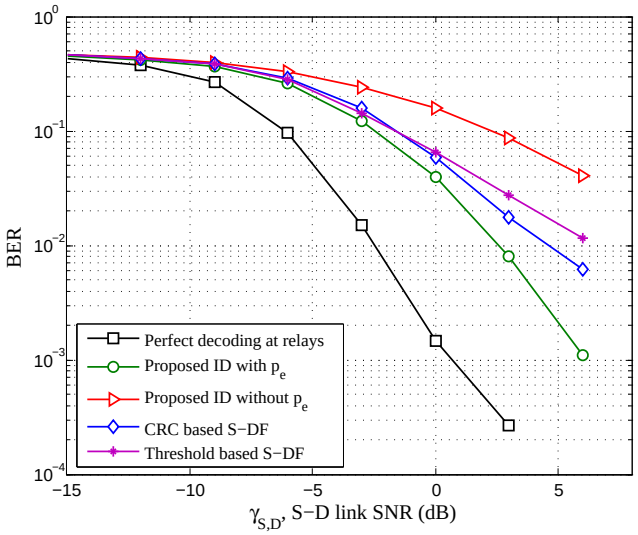

Figure 4.3.: BER versus S-D link SNR with relay-location A in block Rayleigh fading channels and block-length=1024.

Cyclic redundancy check (CRC) based S-DF: relays only forward if they can perfectly decode source's messages and the same iterative decoding at destination as the proposed scheme but without taking p_e into account; 4) *Threshold based S-DF*: relays only forward if decoding errors at relays is less than 15% and the same iterative decoding at destination as the proposed scheme but without taking p_e into account. It is worthwhile to note that all the presented schemes use the same QR-decomposition detection method at relays as described in Sec. II to cancel inter-relay interference.

Fig.4.3 shows BER performances of different schemes with relay-location A. Define $d_{i,j}$ as the distance between the i^{th} and j^{th} nodes. Given the distance between source and destination as $d_{\text{S,D}} = d$, we have $d_{\text{S,R1}} = d_{\text{S,R2}} = d_{\text{R1,D}} = d_{\text{R2,D}} = d$ for relay-location A. As a consequence, based on a simplified suburban area pathloss model with the pathloss exponent equalling to 3.52, SNR relationship in dB among S-D, S-R1, S-R2, R1-D, and R2-D links can be approximated by $\gamma_{\text{S,D}} = \gamma_{\text{S,R1}} = \gamma_{\text{S,R2}} = \gamma_{\text{R1,D}} = \gamma_{\text{R2,D}}$. As shown in Fig.4.3, the scheme of perfect decoding at relays undoubtedly gives the best BER performance and enjoys the full diversity gain of 2. Apart from that, *Proposed ID with* p_e scheme gives the second best BER performance due to the iterative decoding process at destination by taking the error propagation effects into account. By contrast, *Proposed ID without* p_e scheme gives the worst BER performance. The BER performances of two S-DF based schemes are in the middle between *Proposed ID with* p_e scheme and *Proposed ID without* p_e scheme. This is because in this case, the S-DF based schemes prefer to remain silent rather than propagate decoding errors.

In order to generalize the analysis, we also produced BER performances of different schemes for a different relay location (i.e. relay-location B) in Fig.4.4. In this case, given $d_{\text{S,D}} = d$, we have $d_{\text{S,R1}} = d_{\text{S,R2}} = \frac{1}{2}d$ and $d_{\text{R1,D}} = d_{\text{R2,D}} = \frac{3}{4}d$. Then, similar as the setup of relay-location A, the corresponding SNR relationship in dB among S-D, S-R1, S-R2, R1-D, and R2-D links can be approximated by $\gamma_{\text{S,R1}} = \gamma_{\text{S,R2}} = \gamma_{\text{S,D}} + 10.6$ dB and $\gamma_{\text{R1,D}} = \gamma_{\text{R2,D}} = \gamma_{\text{S,D}} + 4.4$ dB. Such location is the case that relays are close to source. As shown in Fig.4.4, the same BER performance trend as Fig.4.3 is presented, where *Proposed ID with* p_e scheme gives the second best BER performance. Comparing Fig.4.3 with Fig.4.4, the BER performance difference between *Proposed ID with* p_e scheme and the conventional S-DF based schemes in Fig.4.4 is larger than the ones in Fig.4.3, where the performance difference in Fig.4.4 can exhibit up to 8 dB gain. This is because, when relays are close to source, their decoding capabilities are increased due to higher received SNR. However, due to the iterative decoding at destination without taking p_e into account, the conventional S-DF based schemes in this case still encounter error propagation effects plus the increased inter-stream interference at destination.

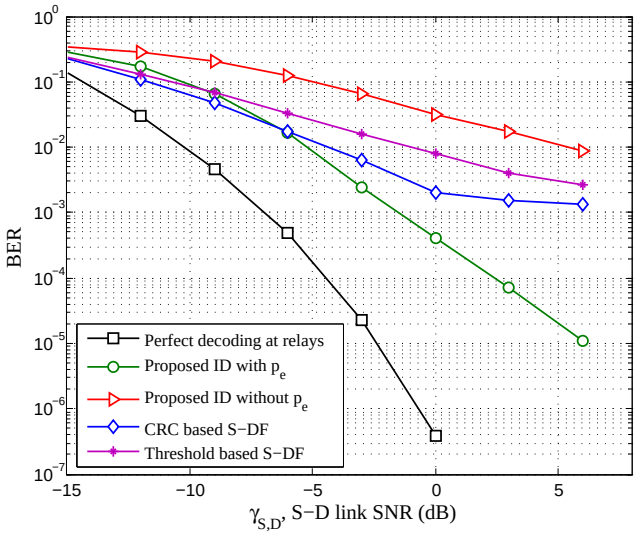

Figure 4.4.: BER versus S-D link SNR with relay-location B in block Rayleigh fading channels and block-length=1024.

4.5 Summary

In this chapter, a successive SIMO erroneous relaying with iterative MAP receiver at destination has been proposed. The proposed scheme allows relays erroneously forward the decoded symbols, and jointly cancels interference and combines diversity at destination. It has been shown that, without extra cost of time delay and signalling overhead, the proposed scheme can exhibit up to 8 dB gain by comparing with the conventional S-DF based schemes especially for relay-location B.

5. Application of RESCUE coding to 802.11 WiFi

5.1 Introduction

In this chapter, we apply the RESCUE JD technique into IEEE 802.11a/g/p standard. In particular, we investigate the impact of utilizing JD together with ARQ. It is shown that even with a very small change in standard, we can achieve about 0.5 dB gain in terms of FER vs SNR.

An open source implementation of orthogonal frequency domain multiplexing (OFDM) [Cha66] transceiver for IEEE 802.11a/g/p networks is available online[1] for GNU Radio[2]. We use this implementation as a basis of our own experiments. The receiver implementation with the fitting for operation with an Ettus USRP N210[3] is described in [BSS+13] and OFDM transmitter using GNU Radio is described for example in [FCV+10].

The high level flow graph of the OFDM tranceiver design in GNU Radio is depicted in Fig. 5.1. The most important blocks in the flow graph are following:

- *TUNTAP PDU*: Creates ethernet connectivity together with *Ethernet Encapsulation* block. This makes possible to use gr-ieee802-11 design as a normal ethernet adapter.
- *OFDM MAC*: Medium Access Control (MAC) block to take care of MAC layer features as described in IEEE 802.11 standard.
- *WiFi PHY Hier*: Hierarchical physical layer block which includes all the physical layer features. This block will be described in more details in section 5.2.1.
- *UHD*, *USRP Sink & UHD*, *USRP Source*: These blocks creates connectivity between flow graph and USRP.

5.2 Implementation

In this section, the physical layer implementation of IEEE 802.11a/g/p is described and the application of JD with minimum modifications is explained. The original IEEE 802.11a/g/p PHY hierarchical block is opened in Fig. 5.2 and it is described in more details in section 5.2.1. The used simulation model including needed changes in standard is described in section 5.2.2.

5.2.1 Original IEEE 802.11a/g/p tranceiver

Fig. 5.2 depicts the GNU Radio flow graph of PHY hierarchical block. Data processing for packet coming from MAC layer is following:

1. OFDM Mapper adds first service field and tail bits to incoming Protocol Data Unit (PDU). After this, data will go through following processing steps: scrambling, convolutional encoding, puncturing and interleaving. Finally processed PDU will be splitted into symbols.
2. *Packer Header Generator* creates signal field. It will be mapped to BPSK symbols inside *Chunks to Symbols* block. Symbols coming out of *OFDM Mapper* block will be mapped using current constellation in the other *Chunks to Symbols* block. Possible symbol constellations are BPSK, QPSK, 16QAM and 64QAM.
3. *OFDM Carrier Allocator* maps incoming symbols and pilot symbols to OFDM subcarriers. There is 48 data symbols in one OFDM symbol. It also appends short and long training sequences into the beginning of the frame.

[1] http://www.ccs-labs.org/software/gr-ieee802-11/
[2] http://gnuradio.org
[3] https://www.ettus.com

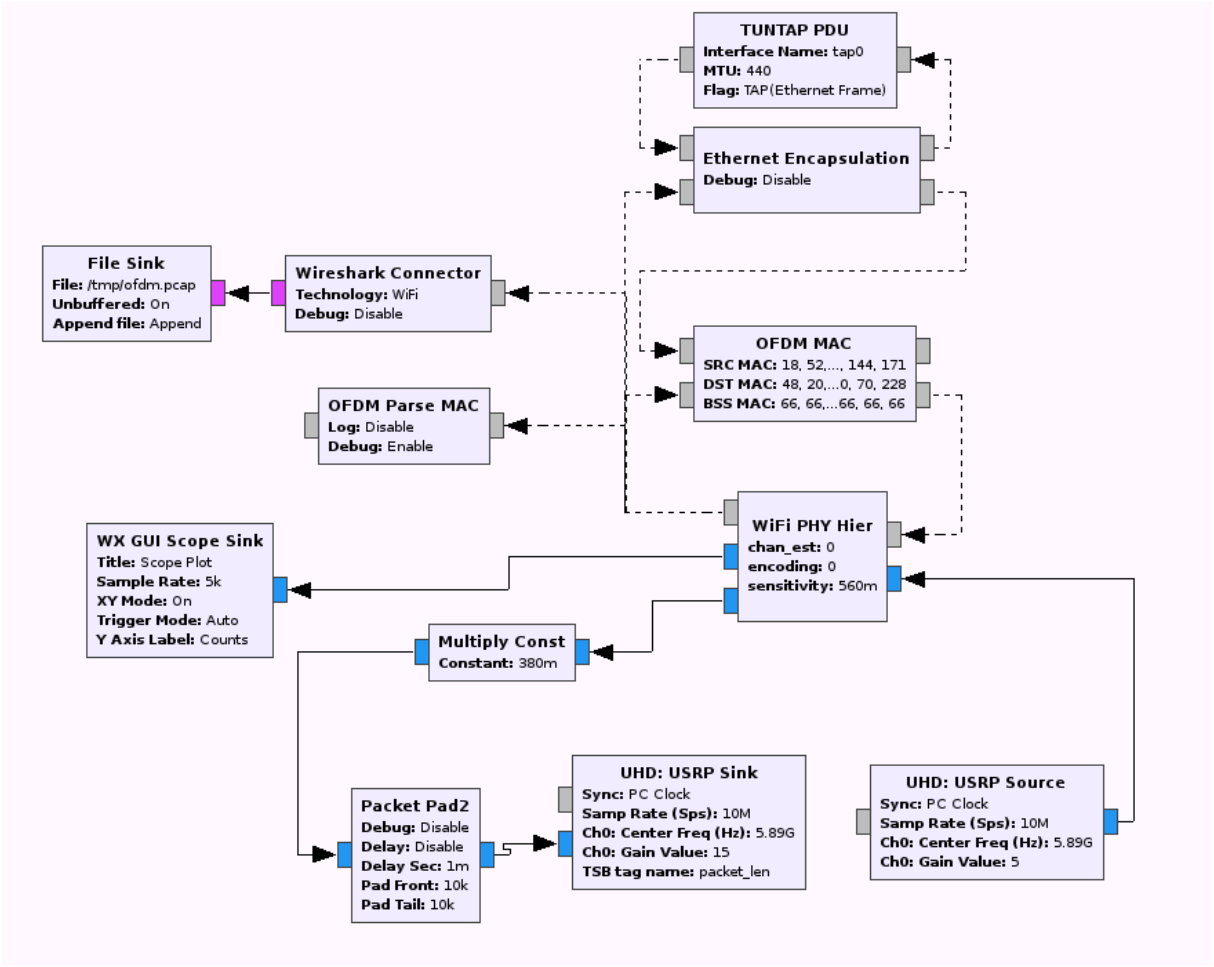

Figure 5.1.: High level flow graph of the OFDM transceiver in GNU Radio.

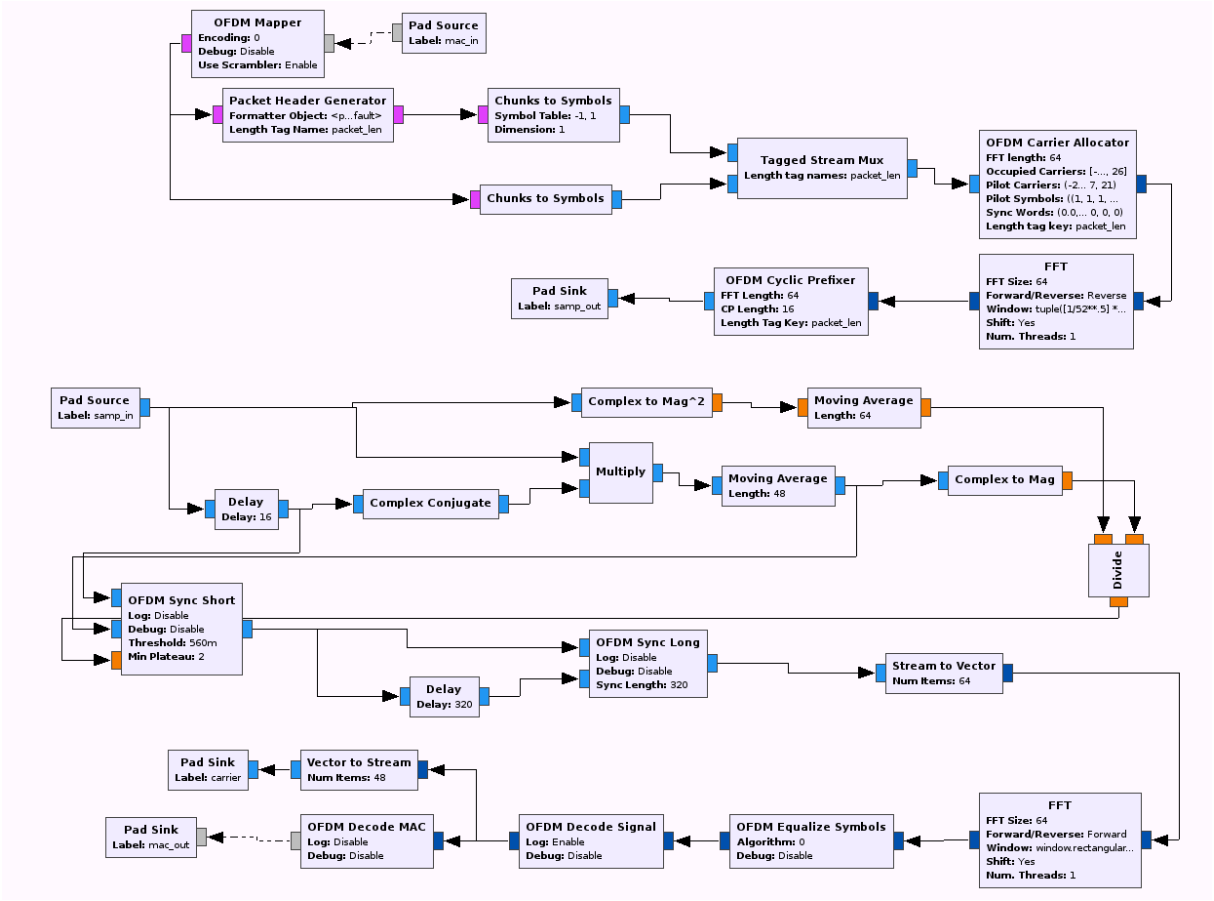

Figure 5.2.: Flow graph of the original physical layer functionalities.

4. At this point packet will go through Inverse Fast Fourier Transform (IFFT). Last step in this processig chain is to add cyclic prefix to OFDM symbols. This will happen inside of OFDM *Cyclic Prefixer* block.

Samples coming from *Pad Source* will go through the following processing:

1. Firstly, signal is fed to a packet detector. Packet detection algorithm is described in [Liu03]. Packet detector blocks will also handle coarse frequency offset correction and remove cyclic prefix.

2. Now sample stream has coarse synchronization and it will go through Fast Fourier Transform (FFT).

3. After FFT, sample stream goes to equalizer. It will correct remaining frequency and phase offset and scale samples to correct amplitude using information from pilot signals. Pilot signals will be removed and only data samples will be outputted.

4. Data samples are now fed to *OFDM Decode Signal* block which decodes the signal. Signal field has rate field and packet length fields.

5. After the signal field is decoded, *OFDM Decode MAC* maps symbols back to bits, deinterleaves, depunctures, decodes and descrambles data and then sends it out to *Pad Sink*.

5.2.2 Simulation Model

In this section, simulation model, changes in standard and test cases are described. To establish RESCUE coding on 802.11 OFDM tranceiver, minimum needed change is random bit-interleaver for payload data. This interleaver will be located before data scrambling. Standard compliant convolutional coding with generator $g_0 = 133_8$ and

$g_1 = 171_8$ is used in implementation.

The simulation model is depicted in Fig. 5.4. It has following new blocks:

- *Rescue decoder*: This block includes all the decoding and demapping functions. It also controls simulations and prints logs.
- *Rescue Packet Generator*: Generates data packets using payload generated by *Rescue decoder*. Generation command also includes desired SNR, code rate, modulation and number of packets to generate.
- *Rescue channel*: AWGN/Rayleigh channel generating Gaussian noise using SNR information.
- *Simulation packet detector*: This block is used to emulate packet detection.

Simulation model has possibility to forward data through OFDM chain and equalizer or just add noise to data symbols. Latter one is used in these simulation to investigate theoretical limits of this technology without nonideal blocks, such as equalizer.

When decoder receives packet it first decodes signal field. If it is successful it decodes the whole packet. If the packet has errors, decoder checks if header's address fields match to the stored addresses. Packets with matching addresses will be added to decode set if any combining is used. In this work, header error rate (HER) will be defined to cover only address part of the header because it is one of the main limiting factor of this technology. If HER increases too much it may mask gains coming from joint decoding.

Test cases selected to study the impact of JD in WiFi are the following:

- Joint decoding using interleaver: Joint decoding is applied to a standard code.
- Combining LLRs after decoding: Just a simple summation of LLRs.
- No combining

Joint decoder structure for *N* frame copies can be seen in figure 5.3. It is worth of noticing that the feedback from the BCJR to the demapper is not effective because BPSK modulation is used in simulations.

5.3 Numerical Results

All the simulations were run over 2000 generated individual packets with 10 retransmitted copies per packet. As mentioned in Section 5.2.2, rate 1/2 convolutional coding with generator $g_0 = 133_8$ and $g_1 = 171_8$ is used together with BPSK modulation. Frame Error Rate (FER) comparison between joint decoding, LLR combining after decoding and no combining for one and two copies can be seen in Fig. 5.5 and for 5 and 10 copies in Fig. 5.6. HER is also plotted to figures. It can be seen from Fig. 5.5 that a small gain is achieved by adding the interleaver and performing iterative joint decoding. From Fig. 5.6, we can observe that the gain is increased when having more copies, reaching up to 0.5 dB with 10 frame copies. As already mentioned in Section 5.2.2, it can be also observed from Fig. 5.6 that HER is restricting the performance of both, combining and JD. In fact, even if ten copies are sent, the number of the copies that are jointly decoded is much less in low SNR regime, because of the erroneous headers.

5.4 Conclusions

As was seen from numerical results, gain achieved by adding interleaver and performing iterative joint decoding gives maximum of 0.5 dB more SNR operating range with high number of retransmissions and less with a fewer number of copies. The limited gain is mainly due to the impact of HER but also due to the fact that the standard code is not designed for iterative processing. Therefore, this topic should be studied further with different modulation

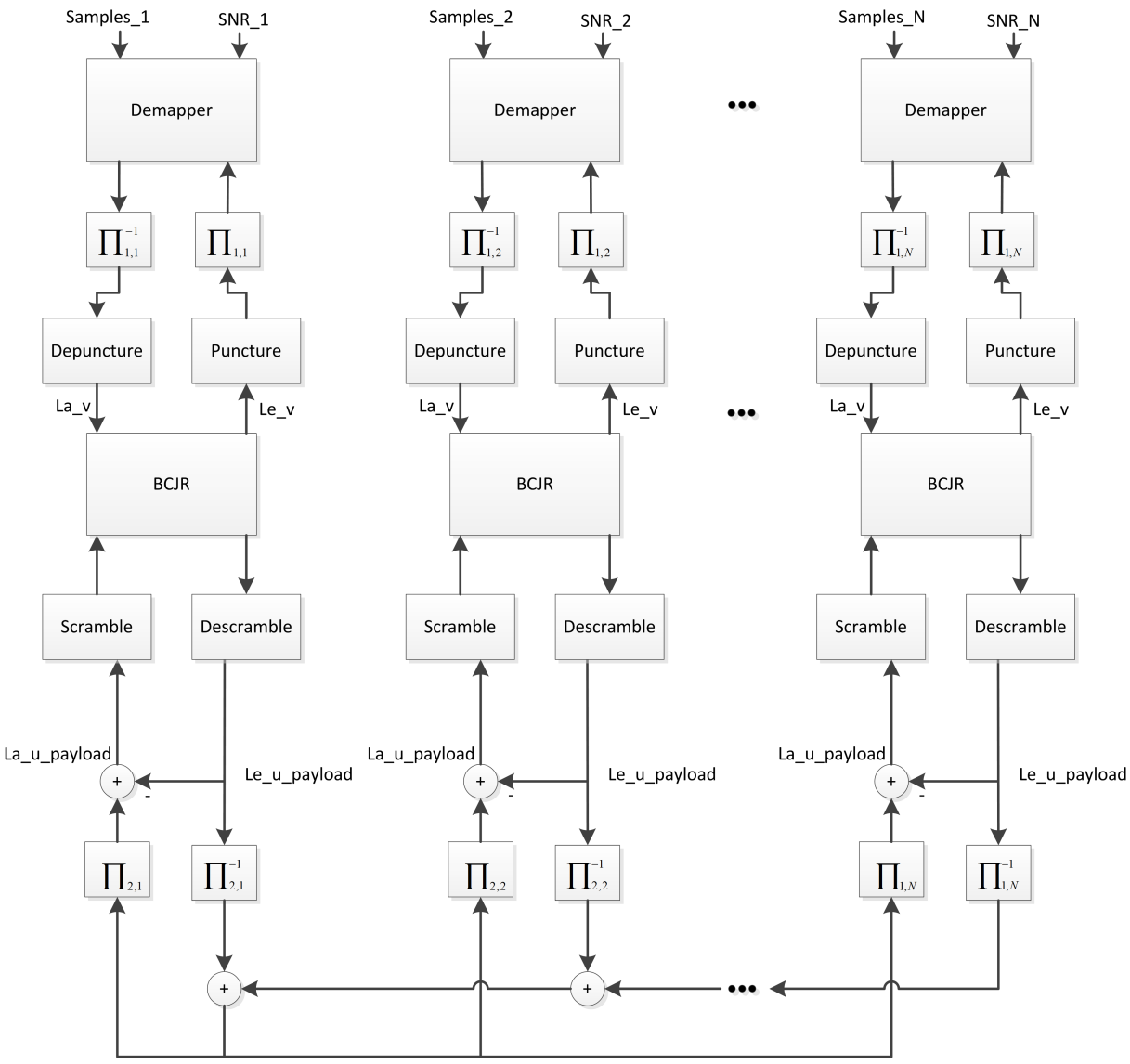

Figure 5.3.: Joint decoder for 802.11 simulation.

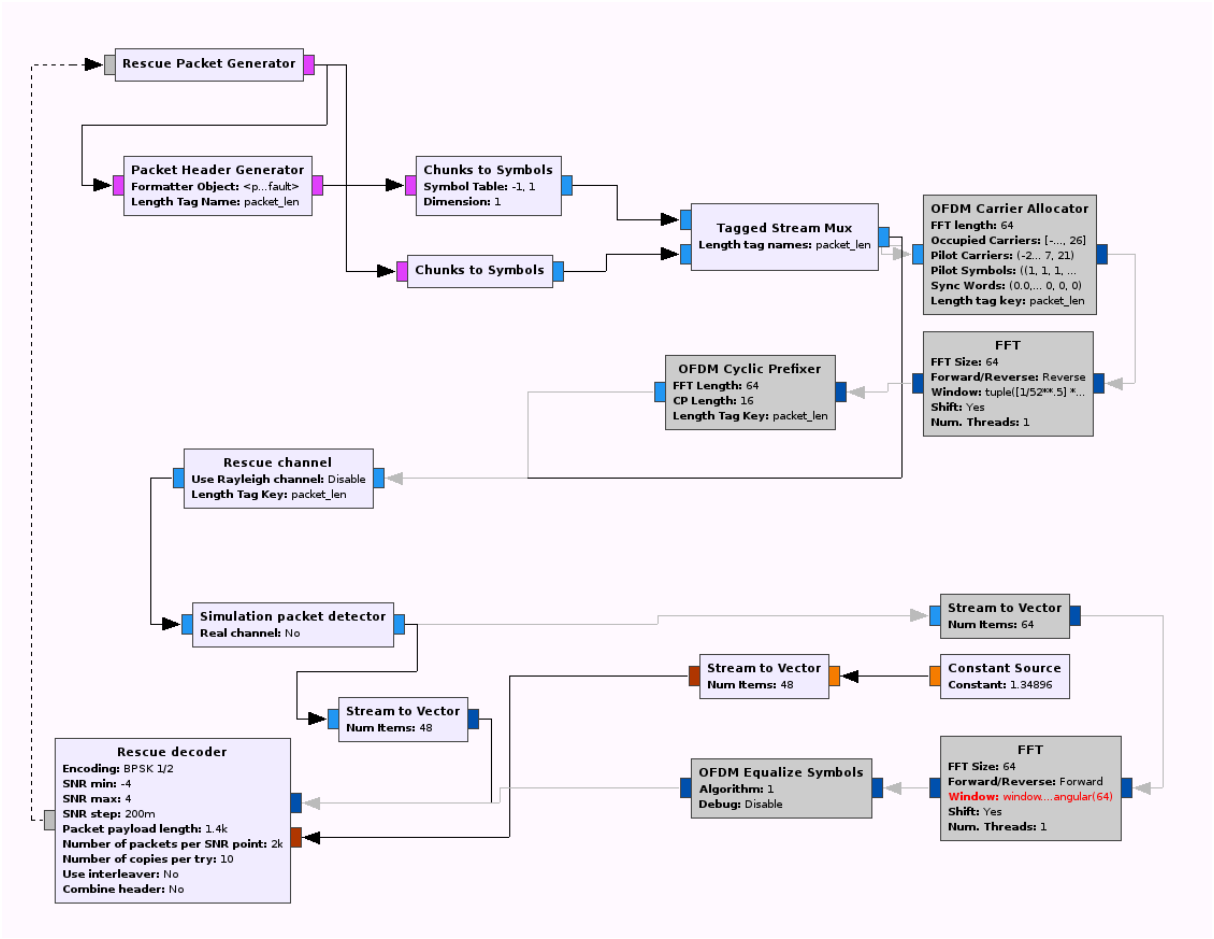

Figure 5.4.: Flow graph of the physical layer including RESCUE functionalities.

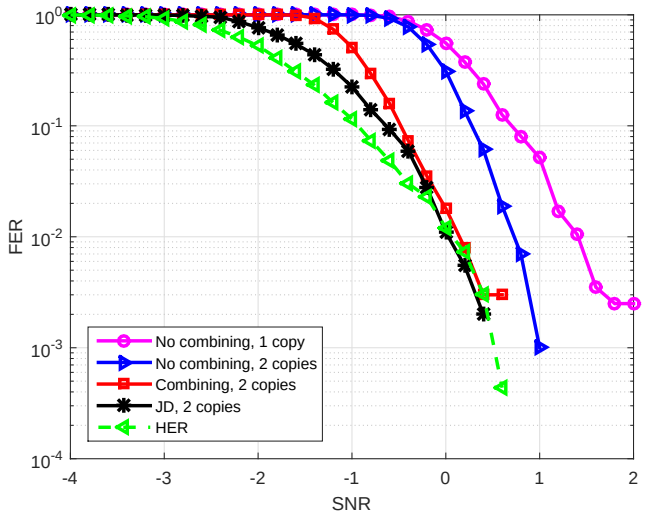

Figure 5.5.: BER results for one and two frame copies.

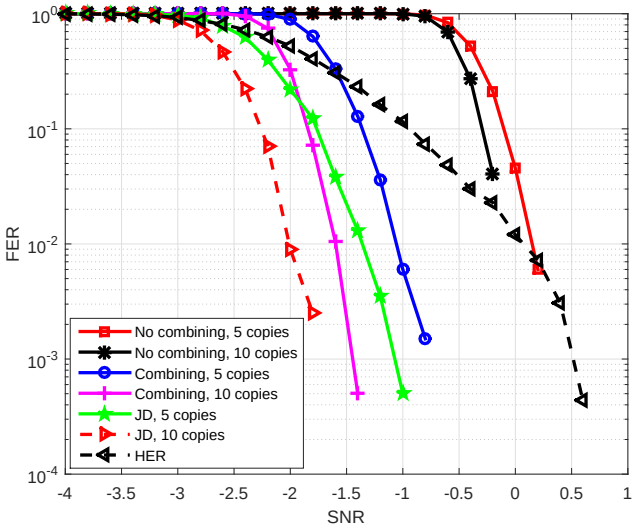

Figure 5.6.: BER results for five and ten frame copies.

and coding schemes and possibly even with different forward error correction codes, such as the code designed for RESCUE.

Even though it would be possible to get more gain by designing better codes for this purpose, 802.11 may be challenging environment for joint decoding because of its nature as interference limited system. Packet corruptions because of collisions may dominate instead of Gaussian noise and for that purpose, JD should be combined with interference cancelation techniques.

6. An Error Rate Model for RESCUE PHY

This chapter presents a link quality model for a wireless communication system with DTC and LF. The model maps the signal-to-interference-plus-noise ratio (SINR) of packet copies received from different links to a mutual information (MI) parameter and, in a second stage, converts it to a block error rate. The model accurately predicts the link-level performance at a low computational complexity and can be therefore used as a physical layer (PHY) abstraction for the computationally-intensive, simulation-based performance evaluation of various functionalities at higher protocol layers or at the system level. In order to illustrate the usage of the proposed model, we show the integration of the model into a protocol level simulator assessing the performance improvements of LF and JD. This work has been published in [THZ+16].

6.1 System Model

A block diagram of a parallel lossy DF relaying model is depicted in Fig. 6.1, where $\mathbf{u}_k = \mathbf{u} \oplus \mathbf{e}_k$ denotes the binary sequence at a relay k after decoding, $\oplus$ indicates modulo 2 addition, $\mathbf{u}$ is the original binary independent identically distributed (i.i.d.) information sequence from the source, and $\mathbf{e}_k = [e_{k,1}, e_{k,2}, \ldots, e_{k,L}]$ is a bit flipping sequence defined as

$$e_{k,n} = \begin{cases} 1, & \text{with probability } p_k, \\ 0, & \text{with probability } 1-p_k, \end{cases} \quad n = 1,2,\ldots,L. \tag{6.1}$$

Each correlated version of the source sequence $\mathbf{u}_k$ is interleaved and encoded by a twofold serially concatenated code at the relay: First, a systematic non-recursive convolution code (SNRCC) and second, a doped accumulator (ACC) [AM12], i.e., memory-1 systematic recursive convolutional code (SRCC) are deployed. The ACC is used to prevent an error floor at the relay decoder [PS06]. Finally, the modulated sequence $\mathbf{s}_k$ is transmitted over a block fading channel, where γ_k is a fading factor and $\mathbf{w}_k$ is Gaussian noise.

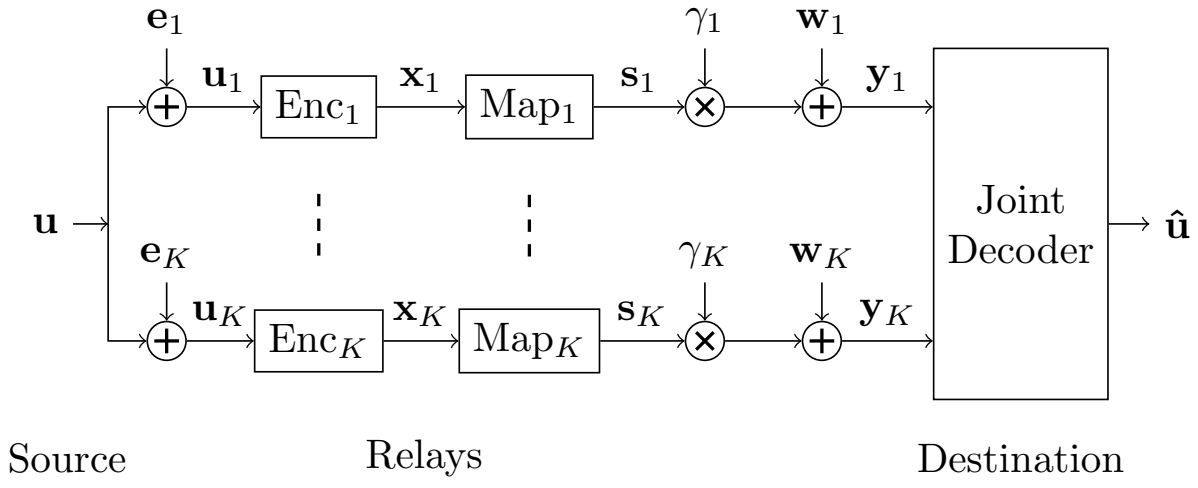

Figure 6.1.: A schematic diagram of a parallel relaying model [D211].

At the destination, soft demapping is applied by calculating the log-likelihood ratio (LLR) $\mathbf{L}_{x_k}$ with the received sequence $\mathbf{y}_k$ and known channel state information. Each relay decoder in Fig. 6.2 has two matching BCJR algorithms [BCJ+74]. In general, the joint decoder is structured in two main parts: (1) the local iteration (LI), where the relay sequence is decoded, and (2) the global iteration (GI), where the information exchange among all relay sequences is performed. In GI the LLR update function [AM12], based on the knowledge of p_k, updates the LLRs $\mathbf{L}^e_{u_k}$ accordingly[1]. If the LLRs $\mathbf{L}^e_{u_k}$ are not improving anymore, the final estimation of $\mathbf{u}$ is determined by hard decision of the sum of all $\mathbf{L}^e_{u_k}$. For a detailed explanation of the joint decoder, we refer to [HZA+13].

[1]The value of p_k can be estimated at the relay and transmitted to the destination or it can be estimated during the decoding process.

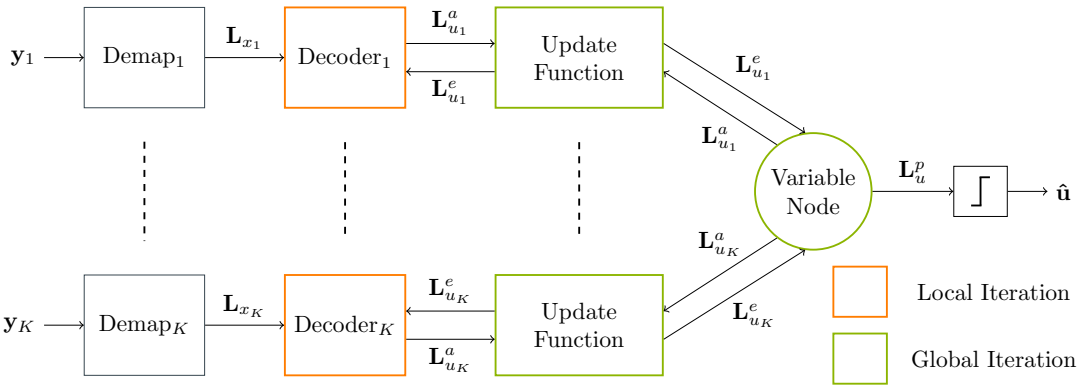

Figure 6.2.: The joint decoding strategy utilizes correlation knowledge among the relays data through global iteration [HZK+15].

6.2 Error Rate Model

The MI-based metric is well suited for the link-level abstraction of the system model where same data is received through multiple parallel links. Fig. 6.3 divides the abstraction model into two components, Blackbox #1 and #2, which illustrate the deterministic and stochastic parts, respectively. The idea is to use the MI metric given by Blackbox #1 to match with simulation based results stored in Blackbox #2. To be more specific, Blackbox #1 compresses a given set of parameters into a one single scalar, which is further mapped with simulation results in Blackbox #2. In the following we describe the content of both parts of the abstraction model.

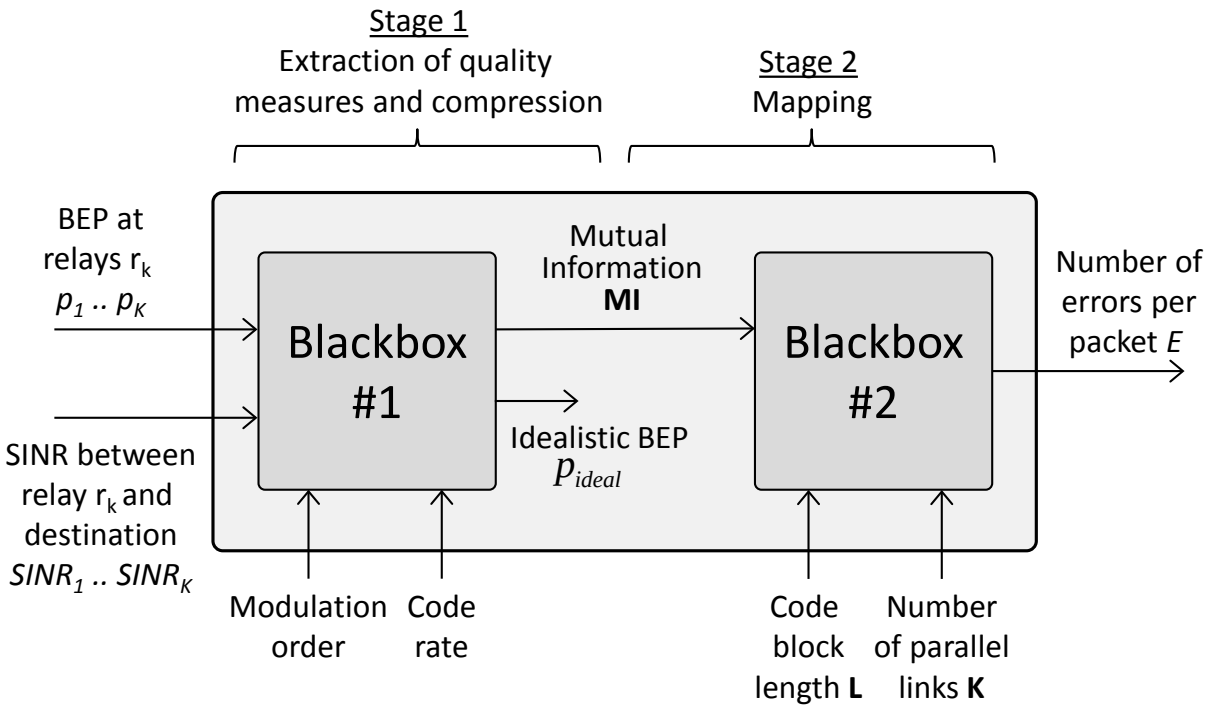

Figure 6.3.: PHY abstraction for link-level performance in multi-path relay networks with LF and joint decoding.

6.2.1 Blackbox #1

Blackbox #1 was originally described in [D211]. The BER after JD at the destination depends on the bit error probability (BEP) at the relay k (p_k), the SINR of the link between relay k and the destination ($SINR_k$), and the

used modulation and coding scheme (MCS). Next, we show how these parameters are mapped to a single scalar MI.

A simplified version of the "achievable rate region" from [ZCH+14] is shown in Fig. 6.4. The figure corresponds to a three-node system model, where the destination receives two copies of the same data packet, one directly from the source and another from a relay node. Here, the relay may be unable to decode correctly, and the resulting BER at the relay is p. The axes R_1 and R_2 represent the scaled channel constellation constrained capacities (CCCs) of the source-to-destination link and the relay-to-destination link, respectively, given by $R_k = \frac{C(\mathscr{M}_k, SINR_k)}{R_c^k \mathscr{M}_k}$, with $C(\mathscr{M}_k, SINR_k)$ being the CCC of AWGN channel of the parallel link k depending on the modulation and $SINR_k$. The scaling is performed with the spectral efficiency depending on the number of bits per symbol $\mathscr{M}_k$ in complex modulation and the channel code rate R_c^k used at the relay k.

Theoretically, if the rate pair falls into the achievable rate region, error-free decoding at the destination is possible. Note that the rate region is information theoretic and independent of the code design and decoder implementation. We assume that the source sequences $\mathbf{u}_1$ and $\mathbf{u}_2$ have full entropy, i.e., $H(\mathbf{u}_1) = 1$ and $H(\mathbf{u}_2) = 1$, respectively.

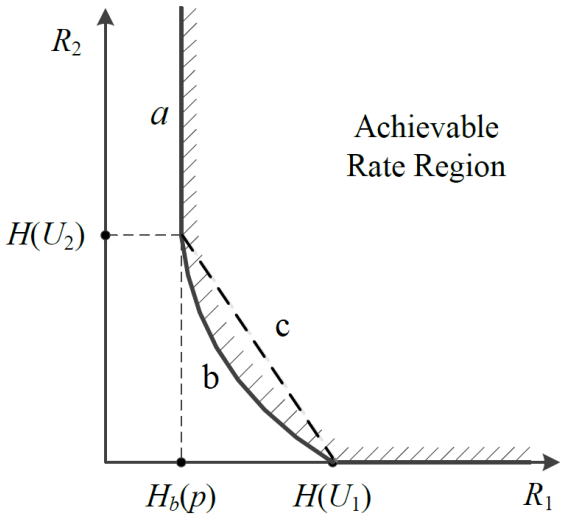

Figure 6.4.: Rate region for a three-node system.

The bound of the admissible rate region consists of the straight line a, i.e. $R_1 + (1 - H_b(p_k)) = 1$ and the curve b. Here $H_b(p_k) = -p_k \log_2 p_k - (1-p_k)\log_2(1-p_k)$ denotes the binary entropy associated with probability p_k. In order to simplify the model, we approximate the curve by the straight c as $R_1 + (1 - H_b(p_k))R_2 = 1$. By combining the two lines, we get an expression for the approximated admissible rate region as

$$R_1 + \min\{1 - H_b(p_k), (1 - H_b(p_k))R_2\} \geq 1. \tag{6.2}$$

We further propose to generalize the combining of MI over any number of parallel incoming links so that

$$\begin{aligned} MI &= \sum_k M_k \\ M_k &= \begin{cases} R_k, & p_k = 0 \\ \min\{(1 - H_b(p_k))R_k, 1 - H_b(p_k)\}, & p_k > 0. \end{cases} \end{aligned} \tag{6.3}$$

In theory, when MI per bit is unity, there are no errors after JD. Note that if there are errors in the transmitter, corresponding MI remains always below unity. Otherwise, MI can get larger values. If all parallel links have suffered of errors before the last hop (a chief executive officer (CEO) problem [HZK+15]), an error floor occurs [WMF15]. Blackbox #1 also calculates the error floor p_{floor} by using the method described in [D121, Sec. 4.1.4.1].

By employing Shannon's source-channel separation theorem [CT91], the distortion (BER) at the output of the receiver can be lower bounded by the inverse of the binary entropy function [ZCH+14] as

$$p_e = H_b^{-1}(1 - MI), \tag{6.4}$$

which equals to zero when $MI \geq 1$. Now, the idealistic BEP p_{ideal} can be approximated as an upper bound of the error floor and MI as

$$p_{\text{ideal}} = \max\{p_e, p_{\text{floor}}\}. \tag{6.5}$$

We call the mapping from the link-specific SINRs and transmitter BERs into the MI and p_{ideal} as Blackbox #1. It employs a very simple deterministic mapping that is independent of the coding and decoding scheme, and requires no simulations. It predicts optimistic performance that corresponds to infinite packet sizes. It is also worth of noticing that due to the summation of MIs in (6.3), the theory assumes that the erroneous bits do not interfere in decoding process, i.e., erroneous bits are treated as erasures.

6.2.2 Blackbox #2

It is well known that in block codes, the number of bit errors per packet is not uniformly distributed. In order to obtain MCS and packet length dependent BER performance results, we propose to concatenate Blackbox #1 with Blackbox #2 that employs a mapping obtained via simulations in the AWGN channel. Note that these results apply also in block fading channels. The idea is to obtain the random packet-by-packet decoding performance in terms of BER. In the following, we will describe the construction of mapping tables used in Blackbox #2 for K parallel links.

6.2.2.1 Construction of simulation tables for Blackbox #2

Since Blackbox #1 is able to do the compression of channel quality measures to a single scalar, we can significantly reduce the number of simulation tables needed. For the simulations, we can perform the following simplifications: set $p_k = 0$ for all k, since p_k is already taken into account when calculating MI through (6.3). Furthermore, since the simulation results and the theoretical results are compared only in terms of the sum of the MIs over the links, we can set $SINR_k = \hat{\gamma}$, $\forall k$, and sweep $\hat{\gamma}$ through an appropriate SINR range. The simulations have to be performed separately for all MCSs considered.

Simulations were performed by sending 10,000 packets (8,000 bits each for QPSK, 8,400 for 16-QAM and multi-rate) through the channel of each parallel link with orthogonal channel access. The output of the simulations was the number of errors in each packet after JD at the destination. Empirically, it was found that the errors are distributed approximately according to a distribution defined as

$$P(\alpha, \mu, \sigma^2) = \alpha\delta(0) + (1-\alpha)\mathcal{N}(\mu, \sigma^2), \tag{6.6}$$

where α is the probability that the number of errors in a packet is zero, $\delta(\cdot)$ is the Dirac delta function, and $\mathcal{N}(\mu, \sigma^2)$ denotes the normal distribution with mean μ and variance σ^2. An intuitive explanation for (6.6) is that α portion of the packets are error-free, and for the remaining part, the error distribution follows Gaussian.

The parameter values $p_k = 0$ and $SINR_k = \hat{\gamma}$ are fed to Blackbox #1 which outputs MI. For this given p_k and $SINR_k$ values, we run simulations and then fit the simulation data to the distribution given above, resulting in numerical values of parameters α, μ, and σ^2 corresponding MI output from Blackbox #1. As a result, we can construct a table with four columns that corresponds to MI, α, μ, and σ^2, respectively.

6.2.2.2 Generation of bit errors using Blackbox

Since the resolution for the MI values listed in the table is finite, linear interpolation can be used to obtain numerical values for the distribution parameters between the quantized points. For the cases where at least one error-free component exists at the relay, errors can be generated directly from (6.6). In the case of CEO problem, there exists an error floor which is composed of uniformly distributed errors which further need to be considered by adding $E = E + E_{floor}$, where E_{floor} is the number of errors induced by error floor. The generation of the number of bit errors E is described in **Algorithm** 1. The operation $E = \max\{0, E\}$ is used to prevent negative values of E. Symbol L at line 13 denotes the length of a block.

Algorithm 1: Bit error generation for multi-path relay networks with LF and JD.

Input parameters $p_1, p_2, \ldots, p_K$,
$SINR_1, SINR_2, \ldots, SINR_K$
Calculate MI using (6.3)
Find α, μ, σ^2 matching the values on the tables with MI
using linear interpolation
Generate uniformly distributed random number $\rho \in [0,1]$
if $\rho > \alpha$ **then**
  Generate E from $\mathcal{N}(\mu, \sigma^2)$
  and choose $E = \max\{0, E\}$.
else
  $E = 0$
end if
Calculate p_{floor} using the method
from [Xia15, Sec. 4.1.4.1]
if $p_{floor} > 0$ **then**
  Initialize $E_{floor} = 0$
  for $i = 1, 2, \ldots, L$ **do**
    Generate uniformly distributed random number
    $\rho_{floor} \in [0,1]$
    if $\rho_{floor} < p_{floor}$ **then**
      $E_{floor} = E_{floor} + 1$
    end if
  end for
  $E = E + E_{floor}$
end if

6.3 Validation

In this section, we will analyze the accuracy of Blackbox in terms of BER and BLER in AWGN channel. Two different MCSs are used: quadrature phase shift keying (QPSK) with channel code rate 1/2 and 16-ary quadrature amplitude modulation (QAM) with channel code rate 3/4. The channel code parameters are shown in Table 6.1. Natural mapping and modified set partitioning mapping (MSP) are used for QPSK and 16-QAM, respectively.

We define four test cases:

- Case 1: QPSK with three parallel links:
  $\mathbf{p} = [p_1, p_2, p_3]$=[0 0 0].
- Case 2: Two parallel links, one uses QPSK and one uses 16-QAM: **p**=[0 0].
- Case 3: QPSK with three parallel links: **p**=[0.01 0.02 0].
- Case 4: QPSK with three parallel links:
  p=[0.01 0.02 0.05].

Cases 1 and 2 represent cases where exactly the same data is transmitted through independent links. From the relay network perspective, this means that all routes are error-free before the last hop (relay-destination link). Case 3 is a case where one of the routes is error-free and two of them have suffered from errors before the last hop. Case 4 represents a CEO problem.

Table 6.1.: MCS parameters

	QPSK	16-QAM
Overall rate	1/2	3/4
Inner code	**Doped ACC with puncturing**	
Doping	8	1
Puncture pattern	[0 1]	[0 1]
Inner code rate (after puncturing)	1	1
Memory	1	1
Outer code	CC	CC with puncturing
Polynomial description	{3,2}	{7,5}
Puncture pattern	NA	[1 0 1] for even positions, [1 1 0] for odd
Outer code rate (after puncturing)	1/2	3/4
Memory	1	2

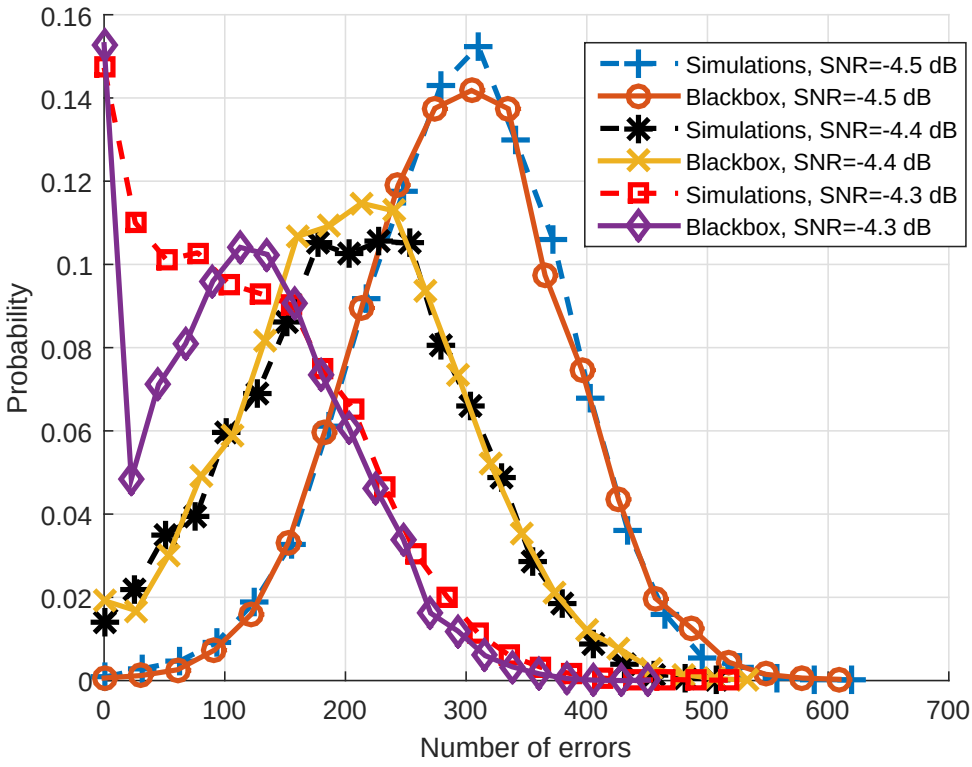

Figure 6.5.: Error distributions for Case 1 obtained by Blackbox and simulations.

The first step is to validate the error distribution defined in (6.6). The error distributions for Case 1 obtained using Blackbox and chain simulations with three SNR values are shown in Fig. 6.5. The SNR values are chosen from the waterfall region, since it is the most difficult region to track. It can be seen that the distributions match very well, although slight deviation is obtained in SNR=-4.3 dB.

Figs. 6.6 and 6.7 show the average BER and BLER, respectively, obtained using Blackbox and through simulations. The value of p_{ideal} is taken directly from Blackbox #1 and $\text{BLER}_{\text{ideal}} = 1-(1-p_{ideal})^L$. We can see that in cases 1

and 2, the curves exactly match. For cases 3 and 4, it can be observed that the result provided by the Blackbox is optimistic compared to the simulations. Possible approaches to improve the accuracy are to improve the JD performance, improve the accuracy of the theoretical results used in Blackbox #1 and/or to find better matching error distributions. However, this investigation to improve the accuracy of the model in Cases 3 and 4 is left as a future study.

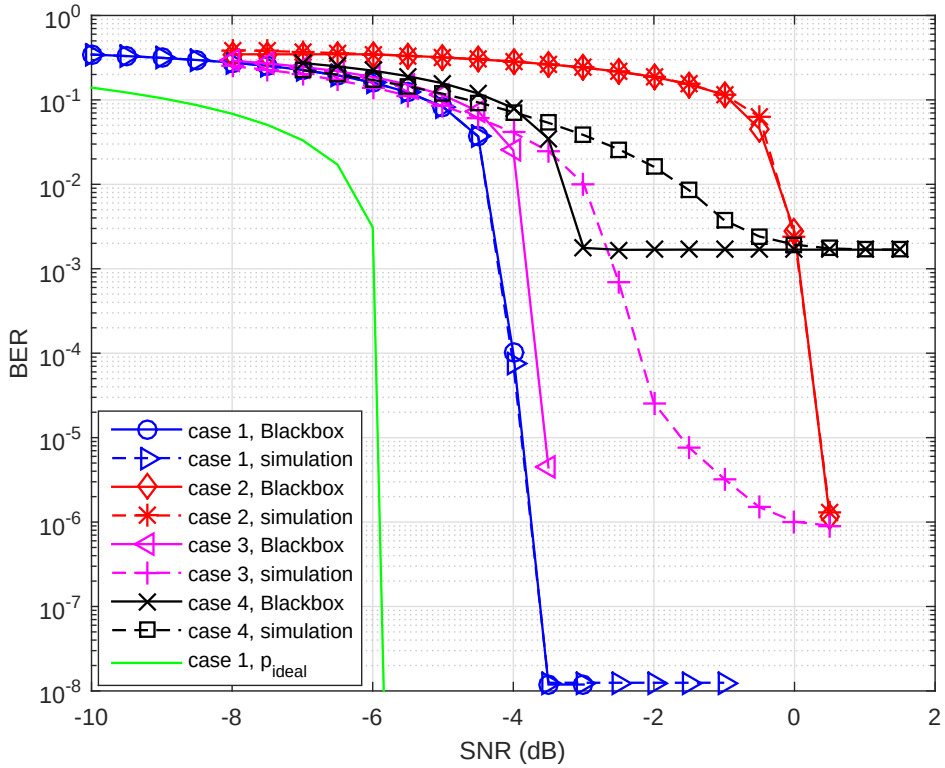

Figure 6.6.: Average BER results obtained by Blackbox and simulations.

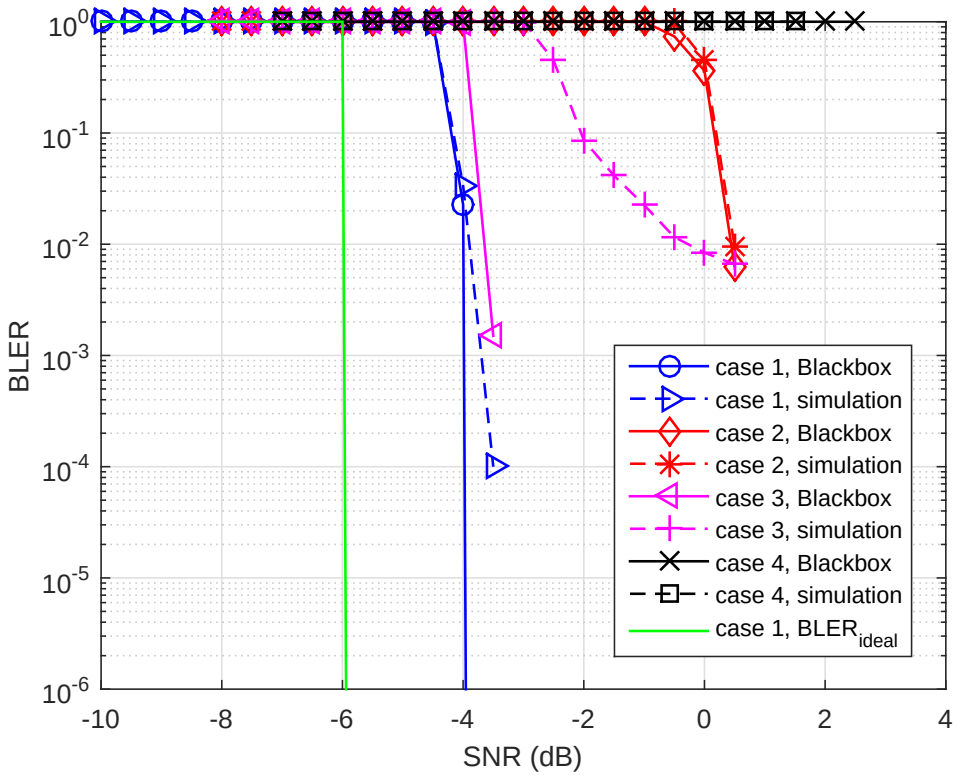

Figure 6.7.: BLER results obtained by Blackbox and simulations.

6.4 Application

We have integrated the Blackbox into the popular ns-3 simulator and carried out a simulation-based performance evaluation for a representative scenario. This section explains the implementation design for the ns-3 enhancements and presents the performance results.

6.4.1 Integration of the Blackbox into Network Simulator ns-3

ns-3 is a discrete-event simulator, which models the operation of the system as a discrete sequence of events in time. Key components of a network based on ns-3 models are nodes, applications, channels and network devices, the latter model the link-level including PHY and MAC. For scalability reasons and to enable simulations at low computational costs, ns-3 implements PHY abstractions to predict the link layer performance. A MI-link quality model has already been integrated into the ns-3 distribution [MMR+12]. However, this model does not consider relaying. Therefore, we have implemented the error rate model for LF and JD and integrated it into ns-3[2].

For our studies we have used the ns-3 *wifi* module, which simulates the IEEE 802.11 PHY and MAC. The integration of the PHY abstraction takes place inside the *WifiPhy* and the *yans* classes, more specifically in the *send* and *receive* functions. We make use of packet tags, a ns-3 feature that allows appending additional information to a packet and thereby to enhance existing protocols by functions for LF and JD.

6.4.2 Simulation Scenario and Results

The network under consideration consists of a single source, multiple (two or three) relays and a single destination. We study the effect of joint decoding and quantify the advantage of using more relays with respect to the reliability.

[2]The implementation of the Blackbox for ns-3 is available as open source at `https://mns.ifn.et.tu-dresden.de/Research/Projects/Pages/RESCUE.aspx`.

The nodes execute a WiFi-like PHY and MAC (IEEE 802.11a) extended by LF and JD. For multi-path packet routing we apply an enhanced version of contention-based geographical forwarding (CBGF) [KFF16]. The channel is modeled by a log-distance path loss with a channel exponent of 3 and Nakagami distribution with shape factor 1, which corresponds to a Rayleigh fading channel. For details of the scenario and models we refer to [KFF16].

We measure the packet success ratio (PSR) – the ratio of successfully received packets at the destination and the sent packets from the source – the number of packet copies (decoding attempts) required for error-free decoding – over the transmit power in dBm, whereas all nodes have the same transmit power. In *LF+JD-On* packets with errors are forwarded at the relays (lossy forwarding – LF) and combined at the destination (joint decoding - JD) whereas in *LF+JD-Off* the relays forward only those packets that are correct and at the destination joint decoding is disabled, thus the destination needs to wait until an error-free packet arrives.

To illustrate the functioning of the Blackbox, we consider the PSR with respect to the number of decoding attempts, which corresponds to the number of received packet copies, whereas the summation over the per-packet-copy PSR yields the overall PSR (Fig. 6.8 top Accumulated).

The PSR grows for the two-copies and three-copies cases (Fig. 6.8 center and bottom) to a maximum and decreases for higher transmit power values. The reason for the decay is that with a high transmit power the destination is able to successfully decode the first arriving packet copy (see Fig. 6.8 top). For three packet copies, at approximately 25 dBm the two curves intersect (Fig. 6.8, bottom) because with *LF+JD-On* the Blackbox was already able to decode the packet correctly with 2 packet copies and does not require additional packet copies, whereas *LF+JD-Off* need to wait for the third error-free packet copy. If we regard the blue curve in Fig. 6.8 as the baseline then the difference between the red and blue curves gives the gain achieved by LF and JD.

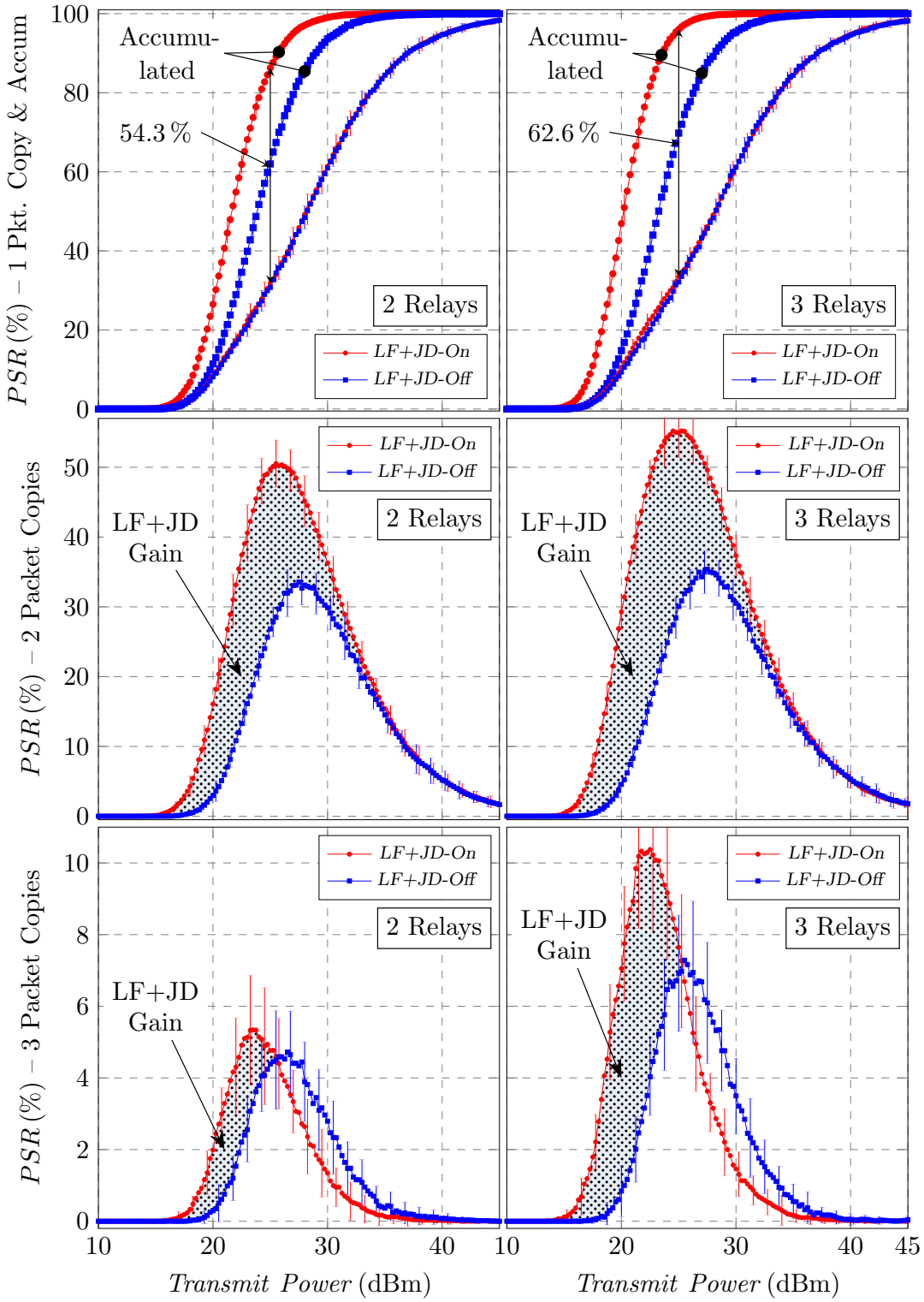

Figure 6.8.: Packet success ratio (PSR) over transmit power [dBm] for the number of decoding attempts (1, 2 or 3 packet copies). The top figures also show the accumulated PSR (sum of all packet copy curves). The error-bars refer to two standard deviations.

6.5 Conclusion

We introduced a model that is capable of predicting the BLER in a wireless communication system with distributed turbo coding, where the destination receives multiple copies of potentially corrupted packets and reconstructs the source information. We have verified the accuracy of the model for the AWGN channel with several modulation and coding schemes. Furthermore, we have demonstrated the application of the error rate model in a protocol simulator and quantified the gains of distributed source coding approach in a state-of-the-art ad hoc routing protocol. The proposed model represents a PHY abstraction that is capable to accurately predict the link-level performance at low computational complexity and can therefore be utilized for the design and performance evaluation of algorithms and protocols that exploit distributed turbo coding as well as for system-level simulation.

7. Conclusion and Future Work

In this deliverable, we have provided comprehensive analytical and simulation results of the coding algorithms used in RESCUE. Furthermore, we have applied the coding algorithms to various frameworks and investigated their applicability in selected cases. Deliverable [D211] presented the basic structure of RESCUE coding/decoding algorithms, however, most of the reported results showed bit error rates (BERs) in AWGN channel, which is indeed enough when investigating the coding gain obtained by the developed coding algorithms. It was shown in [D211] that the RESCUE coding/decoding can achieve BERs less than 2 dB away from the theoretical limits. As the strong error correction capability of RESCUE forward error correction (FEC) code is evident, in this deliverable, we also wanted to address the impact of LF. It is well known, that the majority of the performance increase in cooperative relaying is due to spatial diversity introduced by the relay channels. Therefore, in Chapter 2, we have looked at the performance of the proposed algorithms in fading channels. Specifically, we investigated two scenarios: ,

- TS1: A system with source, relay and destination, where there exist links between every nodes, and
- TS2: A system with source, multiple relays and destination, where the direct link between the source and destination does not exist.

For TS1, we can conclude that if the channel realizations are independent in time, i.e., two successive time slots are uncorrelated, it is often better to use source-destination (SD) link multiple times rather than use the relay channel. However, this requires the availability of the feedback channel. For TS2, we can conclude that LF can operate in wider SNR range than lossless DF.

Chapter 3 described the opportunistic relay selection taking into account the errors occurred in source-relay channels. A statistical learning method for relay selection was also proposed. In the presence of multiple relays, it is important to be able to select the best ones for communication in order to reduce the network traffic. Performance improvements of LF over the lossless DF in terms of required SNR were observed in the considered system model.

Chapter 4 presented a successive SIMO erroneous relaying with iterative MAP receiver for multiplexing loss compensation of HD constrained relaying. Such scheme allows two HD relays alternately serve as transmitter and receiver to continuously transmit data frames for every channel use, and multiple receive antennas can be used for interference cancellation. It was shown that, without extra cost of time delay and signalling overhead, the proposed scheme can reduce the SNR requirement by 8 dB compared with the conventional S-DF based schemes.

Chapter 5 described the application of JD into IEEE 802.11a/g/p standard. The objective was to apply RESCUE coding/decoding with minimal changes to standard. Therefore, we did not consider LF, but we relied on multiple frame copies induced by ARQ. The only change in standard is that the interleaver shuffling the information bits before encoding should be different for each frame copy. It was shown that the FER can be decreased with a cost of increased complexity at the receiver. Even though it would be possible to get even more gain by designing better codes for this purpose, 802.11 may be challenging environment for joint decoding because of its nature as interference limited system. Packet corruptions because of collisions may dominate instead of Gaussian noise and for that purpose, JD should be combined with interference cancelation techniques.

Chapter 6 described the RESCUE PHY abstraction. The model maps the SINR of packet copies received from different links to a mutual information parameter and, in a second stage, converts it to a block error rate. The proposed model is able to accurately predict the link-level performance at low computational complexity and can therefore be utilized for the design and performance evaluation of algorithms and protocols that exploit distributed turbo coding as well as for system-level simulation.

Theoretical results reported in Chapter 2 shows that in TS1, where the relay is placed on the line between source and relay, the optimal relay position is at the midpoint, and the performance is symmetric around it. However, we have observed during the RESCUE project that in interference-free scenario, the RESCUE coding/decoding algorithms have the best performance when the relay is closer to the source and when relay is moved closer to the destination, the performance gets worse w.r.t the theoretical limit. Even though the performance is very good also for lossy frames and naturally we cannot choose the relay positions in RESCUE use cases, this indicates that there are space for improvement. One of the most important parts in JD is the LLR update function that compensates the

loss produced by source-relay link. This function enables the interaction between the two decoders by scaling the LLRs with the BEP between the sequences. RESCUE coding/decoding uses novel estimation algorithms reported in [D211] to find the average BEP. The LLR update function reduces the SNR of all the bits. This raises up a question can we do better than applying this single function to all bits? Is one confidence indicator value about the source-relay channel enough to compensate the loss? The results say that yes, however, does it compensate too much? However, the benefit of the used compensation function is simplicity. Another way to improve the performance of coding/decoding of lossy frames is to investigate the asymmetric scenario. As mentioned earlier, we insist on simplicity and practicality and therefore we use the same code in source and relays. However, we could design better matching codes that adapt with the error probability value at the relay.

Most of the results provided in [D211] and in this deliverable investigate interference-free scenarios. Chapter 4 provided interesting initial results for the case where multiple nodes have an access to the same channel. Unlike in the interference-free system considered earlier, it was observed that the performance improvement in LF-based strategy compared with the lossless relaying increases especially when the relays are closer to the source. This is because, when relays are close to source, their decoding capabilities are increased due to higher received SNR. However, the lossless DF suffers of reduced spatial diversity gain even if only a few bits are erroneous at the relays. The threshold-based S-DF might provide better performance, but the increased multi-stream interference and error propagation effects at the destination will let it lose its performance. This indicates that the multi-antenna interference cancelation based on LF is a promising research direction.

The TS1 results shown in Chapter 2 also indicates that in this simple three-node model with geometric path loss assumption, the availability of the feedback link makes LF meaningless. In other words, in this simple system it is better to retransmit from the source rather than forwarding the lossy frames from the relay. However, ARQ may not be always possible. One of the main use cases in RESCUE is public safety and especially disaster type of situations where infrastructure is partially down. In those cases, we do not necessarily have the control entity, but the source just transmits hoping that someone can hear. The final destination does not necessarily know that someone has transmitted. On the other hand, once the packet has arrived to destination, the network topology may have changed already such that the retransmission is not possible. As already mentioned in Chapter 1, we can conclude that LF is beneficial at least in the following cases:

1. Communications in rapidly changing network topology where the retransmissions are not possible.

2. Communications with low power devices where the nodes need to share the load with each other.

In top of the public safety example described above, case 1 includes examples such as V2V and V2I where car is passing by the relay nodes and the source have only one chance to transmit the data. Another case where the feedback is not available is an asymmetric structure where destination can only receive or there is not enough power to send the feedback. Public safety also includes the security aspect, for which there can be a situation where the source wants to be visible as short time as possible and therefore, avoid retransmissions. Case 2 includes examples such as low power sensor nodes, where we want to balance the power consumption between the sensors.

In the following, we would like to point out some numerical results obtained during the RESCUE project. It has been shown in [AM12], that the coding/decoding algorithms used in RESCUE can reduce the required transmit power at least 1/4 per bit in AWGN channel compared to conventional distributed turbo code. In Chapter 2, we showed that LF can reduce the FER more than 1/2 compared to the lossless DF in fading channels. By using the Erlang formulation presented in Appendix A, we can also have significant capacity and spectral efficiency improvements in specific SNR values.

As a conclusion on RESCUE coding/decoding algorithms, we can state that the code is very simple but remarkably strong performing close to the theoretical limits. As stated already in Chapter 1, this is a completely new code design and up to our best knowledge, there is no existing work with this extend.

8. References

[ABM08] Peter Auer, Harald Burgsteiner, and Wolfgang Maass. "A learning rule for very simple universal approximators consisting of a single layer of perceptrons". In: *Neural Networks* 21.5 (2008), pp. 786–795.

[ABN+] Abdullah Aljohani, Zunaira Babar, Soon Ng, and Lajos Hanzo. "Distributed Source-Channel Coding Using Reduced-Complexity Syndrome-Based TTCM". In: ().

[AM12] Khoirul Anwar and Tad Matsumoto. "Accumulator-Assisted Distributed Turbo Codes for Relay Systems Exploiting Source-Relay Correlation". In: *IEEE Communications Letters* 16.7 (2012), pp. 1114–1117.

[ANH16] Abdulah Jeza Aljohani, Soon Xin Ng, and Lajos Hanzo. "Distributed Source Coding and Its Applications in Relaying-Based Transmission". In: *IEEE Access* 4 (2016), pp. 1940–1970.

[BAP+14] E. Basar, U. Aygolu, E. Panayirci, and H. V. Poor. "A Reliable Successive Relaying Protocol". In: *IEEE Trans. Commun.* 62.5 (May 2014), pp. 1431–1443.

[BCJ+74] L. Bahl, J. Cocke, F. Jelinek, and J. Raviv. "Optimal Decoding of Linear Codes for Minimizing Symbol Error Rate (Corresp.)" In: *IEEE Trans. on Inform. Theory* 20.2 (Mar. 1974), pp. 284–287.

[BS05] Hamid Behroozi and M.R. Soleymani. "Performance of the successive coding strategy in the CEO problem". In: *Global Telecommunications Conference, 2005. GLOBECOM '05. IEEE*. Vol. 3. Nov. 2005, pages. DOI: 10.1109/GLOCOM.2005.1577871.

[BSS+13] Bastian Bloessl, Michele Segata, Christoph Sommer, and Falko Dressler. "An IEEE 802.11a/g/p OFDM Receiver for GNU Radio". In: *ACM SIGCOMM 2013, 2nd ACM SIGCOMM Workshop of Software Radio Implementation Forum (SRIF 2013)*. Hong Kong, China: ACM, Aug. 2013, pp. 9–16. DOI: 10.1145/2491246.2491248.

[Cha66] R. W. Chang. "Synthesis of band-limited orthogonal signals for multichannel data transmission". In: *Bell System Technical Journal* 45 (1966), pp. 1775–1796.

[CT06] Thomas M. Cover and Joy A. Thomas. *Elements of Information Theory*. 2nd. USA: John Wiley & Sons, Inc., 2006.

[CT91] T. M. Cover and J. A. Thomas. *Elements of Information Theory*. New York, USA: John Wiley, 1991.

[D11] ICT-619555 RESCUE Deliverable. *D1.1 – System Scenarios and Technical Requirements*. Tech. rep. May 2014.

[D121] ICT-619555 RESCUE Deliverable. *D1.2.1 – Assessment on Feasibility, Achievability, and Limits*. Tech. rep. Apr. 2015.

[D211] ICT-619555 RESCUE Deliverable. *D2.1.1 – Interim Report of Detailed Coding/Decoding Algorithms and Correlation Estimation Techniques*. Tech. rep. Oct. 2014.

[D23] ICT-619555 RESCUE Deliverable. *D2.3 – Feasibility Assessment in Model Based Environments*. Tech. rep. Nov. 2015.

[D31] ICT-619555 RESCUE Deliverable. *D3.1 – MAC and Routing Architecture and Interfaces Specification*. Tech. rep. Nov. 2014.

[D32] ICT-619555 RESCUE Deliverable. *D3.2 – Report on revised WP3 architecture including simulation results*. Tech. rep. Dec. 2015.

[D33] ICT-619555 RESCUE Deliverable. *D3.3 – Report on implementation of the WP3 architecture*. Tech. rep. Apr. 2016.

[FCV+10] P Fuxjäger, A Costantini, D Valerio, P Castiglione, G Zacheo, T Zemen, and F Ricciato. "IEEE 802.11 p transmission using GNURadio". In: *6th Karlsruhe Workshop on Software Radios (WSR)*. Karlsruhe. 2010, pp. 1–4.

[FWT+07] Y. Fan, C. Wang, J. S. Thompson, and H. V. Poor. "Recovering MultMultiple Loss through Successive Relaying Using Repetition Coding". In: *IEEE Trans. Wireless Commun.* 6.12 (Dec. 2007), pp. 4484–4493.

[GK11] Abbas El Gamal and Young-Han Kim. *Network Information Theory*. New York: Cambridge University, 2011.

[GZ05] J. Garcia-Frias and Ying Zhao. “Near-Shannon/Slepian-Wolf Performance for Unknown Correlated Sources Over AWGN Channels”. In: *IEEE Transactions on Communications* 53.4 (Apr. 2005), pp. 555–559.

[HB07] Jeremiah Hu and Norman C Beaulieu. “Performance analysis of decode-and-forward relaying with selection combining”. In: *Communications Letters, IEEE* 11.6 (2007), pp. 489–491.

[HBP08] J. Haghighat, Hamid Behroozi, and D.V. Plant. “Iterative joint decoding for sensor networks with binary CEO model”. In: *Signal Processing Advances in Wireless Communications, 2008. SPAWC 2008. IEEE 9th Workshop on*. July 2008, pp. 41–45. DOI: 10.1109/SPAWC.2008.4641566.

[HLT12] Y. Hu, K. H. Li, and K. C. Teh. “An Efficient Successive Relaying Protocol for Multiple-Relay Cooperative Networks”. In: *IEEE Trans. Wireless Commun.* 11.5 (May 2012), pp. 1892–1899.

[HYM15] J. Hou, N. Yi, and Y. Ma. “Error Propagation Mitigation by Exploiting Source-Relay Correlation with Limited Channel Feed-Forward Bits”. In: *Proc. IEEE Int. Wksp. Computer Aided Modelling and Design of Communication Links and Networks*. Sept. 2015, pp. 273–277.

[HZA+13] Xin He, Xiaobo Zhou, K. Anwar, and T. Matsumoto. “Estimation of Observation Error Probability in Wireless Sensor Networks”. In: *Communications Letters, IEEE* 17.6 (June 2013), pp. 1073–1076. ISSN: 1089-7798. DOI: 10.1109/LCOMM.2013.042313.130361.

[HZK+15] X. He, X. Zhou, P. Komulainen, M. Juntti, and T. Matsumoto. “A Lower Bound Analysis of Hamming Distortion for a Binary CEO Problem with Joint Source-Channel Coding”. In: *IEEE Transactions on Communications* PP.99 (2015), pp. 1–1. DOI: 10.1109/TCOMM.2015.2499179.

[KFF16] S. Kühlmorgen, A. Festag, and G. Fettweis. “Exploiting Distributed Source Coding for Multi-hop Routing in Wireless Ad Hoc Networks”. In: *IEEE VTC Spring ’16*. Nanjing, China, May 2016, p. 6.

[Lee97] Charles Lee. *Convolutional coding: fundamentals and applications*. Artech House Publishers, 1997.

[LH09] K. Lee and L. Hanzo. “MIMO-Assisted hard versus soft decoding-and-Forwarding for network coding aided relaying systems”. In: *IEEE Trans. Wireless Commun.* 8.1 (Jan. 2009), pp. 376–385.

[Liu03] Chia-Horng Liu. “On the design of OFDM signal detection algorithms for hardware implementation”. In: *Global Telecommunications Conference, 2003. GLOBECOM ’03. IEEE*. Vol. 2. Dec. 2003, 596–599 Vol.2. DOI: 10.1109/GLOCOM.2003.1258308.

[MMR+12] Marco Mezzavilla, Marco Miozzo, Michele Rossi, Nicola Baldo, and Michele Zorzi. “A Lightweight and Accurate Link Abstraction Model for the Simulation of LTE Networks in NS-3”. In: *ACM MSWIM ’12*. Paphos, Cyprus, Oct. 2012, pp. 55–60.

[OS04] T. J. Oechtering and A. Sezgin. “A new Cooperative Transmission Scheme using the Space-Time Delay Code”. In: *Proc. ITG Wksp. Smart Antennas*. Mar. 2004, pp. 41–48.

[PS06] S. Pfletschinger and F. Sanzi. “Error Floor Removal for Bit-Interleaved Coded Modulation with Iterative Detection”. In: *Wireless Communications, IEEE Transactions on* 5.11 (Nov. 2006), pp. 3174–3181. ISSN: 1536-1276. DOI: 10.1109/TWC.2006.05163.

[QCM15] Shen Qian, Meng Cheng, and Tad Matsumoto. “Outage based power allocation for a lossy-forwarding relaying system”. In: *Communication Workshop (ICCW), 2015 IEEE International Conference on*. IEEE. 2015, pp. 2139–2144.

[QZH+ed] S. Qian, X. Zhou, X. He, M. Juntti, and T. Matsumoto. “Outage Analysis for Lossy-Forward Relaying: Impact of Line-of-Sight Component”. In: (2015, submitted). ISSN: 0018-9448. DOI: 10.1109/TIT.2005.853304.

[Rap+96] Theodore S Rappaport et al. *Wireless communications: principles and practice*. Vol. 2. Prentice Hall PTR New Jersey, 1996.

[RYA11] A. Razi, K. Yasami, and A. Abedi. “On minimum number of wireless sensors required for reliable binary source estimation”. In: *Wireless Communications and Networking Conference (WCNC), 2011 IEEE*. Mar. 2011, pp. 1852–1857. DOI: 10.1109/WCNC.2011.5779415.

[SZN11] L. Sun, T. Zhang, and H. Niu. “Inter-Relay Interference in Two-Path Digital Relaying Systems: Detrimental or Beneficial?” In: *IEEE Trans. Wireless Commun.* 10.8 (Aug. 2011), pp. 2468–2473.

[Ten01] Stephan Ten Brink. “Code doping for triggering iterative decoding convergence”. In: *Information Theory, 2001. Proceedings. 2001 IEEE International Symposium on*. IEEE. 2001, p. 235.

[THZ+16] Valtteri Tervo, Xin He, Xiaobo Zhou, Petri Komulainen, Sebastian Kühlmorgen, Albrecht Wolf, and Andreas Festag. "An Error Rate Model of Relay Communications with Lossy Forwarding and Joint Decoding". In: *IEEE ICC '16*. Kuala Lumpur, Malaysia, May 2016, p. 6.

[VHK04] H. Vikalo, B. Hassibi, and T. Kailath. "Iterative Decoding for MIMO Channels Via Modified Sphere Decoding". In: *IEEE Trans. Wireless Commun.* 3.6 (Nov. 2004), pp. 2299–2311.

[VZ03] M.C. Valenti and Bin Zhao. "Distributed turbo codes: towards the capacity of the relay channel". In: *Vehicular Technology Conference, 2003. VTC 2003-Fall. 2003 IEEE 58th*. Vol. 1. Oct. 2003, 322–326 Vol.1. DOI: 10.1109/VETECF.2003.1285032.

[WFT+09] C. Wang, Y. Fan, J. S. Thompson, and H. V. Poor. "A Comprehensive Study of Repetition-Coded Protocol in Multi-User Multi-Relay Networks". In: *IEEE Trans. Wireless Commun.* 8.8 (Aug. 2009), pp. 4329–4339.

[WMF15] Albrecht Wolf, Maximilian Matthe, and Gerhard Fettweis. "Improved Source Correlation Estimation in Wireless Sensor Networks". In: *IEEE ICC '15*. London, UK, June 2015, pp. 2121–2126.

[WTG+11] H. Wicaksana, S. H. Ting, Y. L. Guan, and X.-G. Xia. "Decode-and-Forward Two-Path Half-Duplex Relaying: Diversity-Multiplexing Tradeoff Analysis". In: *IEEE Trans. Commun.* 59.7 (July 2011), pp. 1985–1994.

[Xia15] Xiaobo Zhou et al. *Deliverable D1.2.1, Assessment on Feasibility, Achievability, and Limits V1.0, ICT-619555 RESCUE*. Apr. 2015.

[YG11] R. Youssef and A. Graell i Amat. "Distributed Serially Concatenated Codes for Multi-Source Cooperative Relay Networks". In: 10.1 (Jan. 2011), pp. 253–263. ISSN: 1536-1276. DOI: 10.1109/TWC.2010.102810.100422.

[YMH+15] N. Yi, Y. Ma, J. Hou, and R. Tafazolli. "Symbol-level selective decode-forward relaying for uncoordinated dense wireless networks". In: *Proc. IEEE Int. Wksp. Computer Aided Modelling and Design of Communication Links and Networks*. Sept. 2015, pp. 283–287.

[ZCA+12] Xiaobo Zhou, Meng Cheng, Khoirul Anwar, and Tad Matsumoto. "Distributed joint source-channel coding for relay systems exploiting source-relay correlation and source memory". In: *EURASIP Journal on Wireless Communications and Networking* 2012:260 (2012).

[ZCH+14] Xiaobo Zhou, Meng Cheng, Xin He, and Tad Matsumoto. "Exact and Approximated Outage Probability Analyses for Decode-and-Forward Relaying System Allowing Intra-Link Errors". In: *IEEE Transactions on Wireless Communications* 13.12 (2014), pp. 7062–7071.

[ZHA+12] Xiaobo Zhou, Xin He, Khoirul Anwar, and Tad Matsumoto. "GREAT-CEO: larGe scale distRibuted dEcision mAking Techniques for Wireless Chief Executive Officer Problems". In: *IEICE Trans. on Comm., Special Section on Coding and Coding Theory-Based Signal Processing for Wireless Communications* E95-B.12 (2012), pp. 3654–3662.

Appendix A Converting FER results into Erlang

The Erlang B formula determines the probability that a call is blocked and is a measure of the grade of service for a trunked system which provides no queuing for blocked calls. The Erlang B formula is given by [Rap+96]

$$P_b = \frac{\frac{E^m}{m!}}{\sum_{i=0}^{m} \frac{E^i}{i!}}, \tag{A.1}$$

where m is the number of parallel resources, $E = \lambda h$ is the offered traffic, λ is the mean arrival rate, and h is the mean call holding time. The FER and the mean call holding time is related as

$$h = \frac{1}{FSR} = \frac{1}{1 - FER}, \tag{A.2}$$

where FSR denotes frame success rate.

AWGN Example

Consider Fig. 3-21 in [D23]. At SNR=1.6 dB, the FERs for lossy and lossless schemes are 0.138 and 0.98, respectively. Let $m = 1$ and $P_b = 0.03$. Using A.1 and A.2 we get the call arrival rates 0.027 and $6.19 \cdot 10^{-4}$, i.e., lossy forwarding increases the Erlang capacity in the SNR 43.1 times.